LBL-7238

$\pi\pi$ SCATTERING BY POLE EXTRAPOLATION METHODS

Lawrence Berkeley Laboratory
University of California
Berkeley, California 94720

Fredrick W. Lott, III
Thesis

December 9, 1977

*Prepared under the auspices of the U. S. Energy Research and Development Administration under Contract W-7405-ENG-48

$\pi\pi$ SCATTERING BY POLE EXTRAPOLATION METHODS

Fredrick Wilbur Lott, III
Ph.D. Thesis

Lawrence Berkeley Laboratory
University of California
Berkeley, California 94720

December 1977

ABSTRACT

A 25-inch hydrogen bubble chamber was used at the Lawrence Berkeley Laboratory Bevatron to produce 300,000 pictures of π^+p interactions at an incident momentum of the π^+ of 2.67 GeV/c. The 2-prong events were processed using the FSD and the FOG-CLOUDY-FAIR data reduction system. Events of the nature $\pi^+p \to \pi^+p\pi^o$ and $\pi^+p \to \pi^+\pi^+n$ with values of momentum transfer to the proton of $-t \leq 0.238$ GeV^2 were selected. These events were used to extrapolate to the pion pole ($t = m_\pi^2$) in order to investigate the $\pi\pi$ interaction with isospins of both T=1 and T=2. Two methods were used to do the extrapolation: the original Chew-Low method developed in 1959 and the Durr-Pilkuhn method developed in 1965 which takes into account centrifugal barrier penetration factors. At first it seemed that, while the Durr-Pilkuhn method gave better values for the total $\pi\pi$ cross section, the Chew-Low method gave better values for the angular distribution. Further analysis, however, showed that if the requirement of total OPE (one-pion-exchange) were dropped, then the Durr-Pilkuhn method gave more reasonable values of the angular distribution as well as for the total $\pi\pi$ cross section.

To My Parents

Acknowledgments

I am thankful to my research advisor, Dr. Robert P. Ely, and the chairman of my thesis committee, Dr. Robert W. Birge, for their generosity with their time and their encouragement. I thank the other two members of my thesis committee, Drs. Geoffrey F. Chew and Derrick Lehmer, for their thoughtful comments on the manuscript. I appreciate the helpful suggestions of and many interesting discussions with Drs. George Gidal and William B. Michael and Mr. Philip R. Hanson. The Ely Group has provided a warm intellectual environment making my student days at the Lawrence Berkeley Laboratory pleasant ones. I am grateful to Peggy Fox for her careful typing of the manuscript. I thank the scanning and measuring staff and other support personnel whose efforts were indispensable to the completion of this experiment. Last, but not least, I am especially grateful to my family and friends for all their encouragment and support.

Table of Contents

List of Figures

List of Tables

I. Introduction

During the past decade there has been considerable interest, both theoretical and experimental, in the $\pi\pi$ elastic interaction. It has been impossible, however, to do $\pi\pi$ scattering directly due to the short half-life of the pion. Pions don't last long enough to be good experimental targets. Hence, we must content ourselves with indirect methods to determine the nature of the $\pi\pi$ interaction.

Such methods are available. They are known as the pole extrapolation methods. The first of these was developed by Chew and Low[1] in 1959. These pole extrapolation methods operate in the following manner. One looks at the reactions $\pi N \rightarrow \pi\pi N$. Each of the nucleons is surrounded by a cloud of virtual pions. At small values of momentum transfer to the nucleon ($\Delta^2 = -t$ small, where $t=(p_{Nf} - p_{Ni})^2$) the beam pion interacts with one of the virtual pions in the nucleon's pion cloud as shown in Fig. 1.

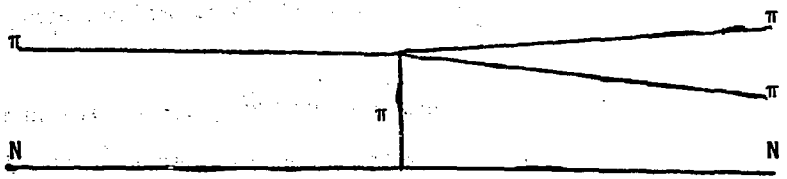

Fig. 1

There is a small amount of momentum transfer when the pion just glances off the nucleon. Then the data for $\pi N \rightarrow \pi\pi N$ is extrapolated, as a function of momentum transfer, to the pion pole ($t=m_\pi^2$). This is the point at which the pion propagator ($\frac{1}{m_\pi^2 - t}$) becomes infinite. In other words, the virtual pion has been converted into a real pion. Of course this pole lies outside the physical region for the reaction $\pi N \rightarrow \pi\pi N$. But the extrapolated

data is able to tell us something about the $\pi\pi$ interaction.

When the data are compared with the Chew-Low formula, however, the fit is not very good as a function of momentum transfer. This poor fit seems to be due to the centrifugal barrier penetration factors described by Blatt and Weisskopf.[2] Hence in 1965 Durr and Pilkuhn[3] introduced some form factors into the extrapolation based on the centrifugal barrier penetration factors. With these form factors it is possible to fit the data better in the physical region. At least it is possible to fit the quantity that is extrapolated to find $\sigma_{\pi\pi}$. These two extrapolation methods are described further in Section II.

It is the purpose of this experiment to compare the Chew-Low and Durr-Pilkuhn extrapolation methods. We will find that the Durr-Pilkuhn method gives more reasonable values for $\sigma_{\pi\pi}$ than the Chew-Low method. On the other hand the Chew-Low method appears to give more reasonable values for the angular distribution of $\pi\pi$ scattering if one assumes one pion exchange (OPE).

The data for this experiment come from 300,000 pictures taken in the 25" bubble chamber at the Berkeley Bevatron. The run used a π^+ beam at a momentum of 2.67 GeV/c. The target was the protons in the hydrogen bubble chamber. The reaction investigated is $\pi^+p \to \pi^+\pi^o p$ which in the spirit of the extrapolation procedure is a function of the I=1 and I=2 $\pi\pi$ amplitude. The $\pi\pi$ invariant mass lies mostly in the region of the ρ^+ meson in the reaction $\pi^+\pi^o \to \rho^+ \to \pi^+\pi^o$.

II. Theoretical Models

A. Chew-Low Extrapolation

In 1959 Chew and Low developed a model by which the reaction aN → bcN could be used to predict the cross sections for the reaction ax → bc. Here x is the exchanged particle in the former reaction. This model is based on the idea that when there is low momentum transfer to the nucleon, i.e., when the particle a just glances off the nucleon, then the particle a interacts with the exchanged particle and converts the latter from a virtual particle to a real particle.

In the case of the reaction $\pi^+p \to \pi^+\pi^0p$ they predict that we can determine the cross section for the reaction $\pi^+\pi^0 \to \pi^+\pi^0$ in the following manner

$$\frac{\partial^2\sigma}{\partial p^2 \partial\omega^2} \xrightarrow[p^2 \to -\mu^2]{} \frac{f^2}{2\pi} \frac{p^2/\mu^2}{(p^2+\mu^2)^2} \frac{[\omega(\tfrac{1}{4}\omega^2-\mu^2)^{\frac{1}{2}}]}{q_{1L}^2} \sigma_{\pi^+\pi^0}$$

where $f^2 = 0.081$ is the coupling factor, q_{1L} is the laboratory momentum of the beam pion, μ^2 is the mass of the exchanged π^0, σ is the cross section for the reaction $\pi^+p \to \pi^+\pi^0p$, $\sigma_{\pi^+\pi^0}$ is the cross section for elastic $\pi^+\pi^0$ scattering, ω is the effective mass of the $\pi^+\pi^0$ system, and $p^2 = \Delta^2$ is the momentum transfer to the nucleon.

If we arrange the terms so that $\sigma_{\pi^+\pi^0}(\omega)$ appears on the left hand side, then we have

$$\sigma_{\pi^+\pi^0}(\omega) = \lim_{\Delta^2 \to -\mu^2} \frac{-\mu^2}{\Delta^2} \frac{-2\pi}{f^2} \frac{q_{1L}^2}{\omega(\tfrac{1}{4}\omega^2-\mu^2)^{\frac{1}{2}}} (\Delta^2+\mu^2)^2 \frac{\partial^2\sigma}{\partial\Delta^2\partial\omega^2}$$

In order to find the angular distribution, we want to differentiate both sides by cosθ. So we have

$$\frac{\partial\sigma_{\pi^+\pi^0}(\omega)}{\partial\cos\theta} = \lim_{\Delta^2 \to -\mu^2} \left(\frac{-\mu^2}{\Delta^2}\right)\left(\frac{-2\pi}{f^2}\right) \frac{q_{1L}^2}{\omega(\tfrac{1}{4}\omega^2-\mu^2)^{\frac{1}{2}}} (\Delta^2+\mu^2)^2 \frac{\partial^3\sigma}{\partial\Delta^2\partial\omega^2\partial\cos\theta}$$

In order to simplify this expression let us define

$$F(W,\omega\,\Delta^2) = -\frac{2\pi}{f^2}\,\frac{q_{lL}^2}{\omega(\frac{1}{2}\omega^2-\mu^2)^{\frac{1}{2}}}\,(\Delta^2+\mu^2)^2\,\frac{\partial^2\sigma}{\partial\Delta^2\partial\omega^2}$$

and

$$F(W,\omega,\Delta^2,\cos\theta)=-\frac{2\pi}{f^2}\,\frac{q_{lL}^2}{\omega(\frac{1}{2}\omega^2-\mu^2)^{\frac{1}{2}}}\,(\Delta^2+\mu^2)^2\,\frac{\partial^3\sigma}{\partial\Delta^2\partial\omega^2\partial\cos\theta}$$

then we may write

$$\sigma_{\pi^+\pi^0}(\omega) = \lim_{\Delta^2\to-\mu^2}\left(\frac{-\mu^2}{\Delta^2}\right)F(W,\omega,\Delta^2)$$

and

$$\frac{\partial\sigma_{\pi^+\pi^0}(\omega)}{\partial\cos\theta} = \lim_{\Delta^2\to-\mu^2}\left(\frac{-\mu^2}{\Delta^2}\right)F(W,\omega,\Delta^2,\cos\theta)$$

In these expressions F vanishes for $\Delta^2=0$ in such a way that $\frac{-\mu^2}{\Delta^2}$ F remains finite. Now it is possible to fit $\frac{-\mu^2}{\Delta^2}$ F to the data in the physical region and extrapolate to the pole ($\Delta^2=-\mu^2$). In this experiment a linear fit was used ($-\frac{\mu^2}{\Delta^2}F = a+b\,\Delta^2$). The quantities a and b were determined by minimizing the χ^2.

B. The Durr-Pilkuhn Model

In 1965 Durr and Pilkuhn[3] developed a model to fit the data in the physical region. The Chew-Low polynomial extrapolation did not fit the data in the physical region very well. Hence a theory was needed to describe the data. The Durr-Pilkuhn model introduces some form factors derived from the centrifugal barrier penetration factors described by Blatt and Weisskopf.[2]

For the reaction $\pi^+ p \to \rho^+ p$, these form factors become

$$G(\omega,t,c,R_p,R_\rho) = \frac{c-t}{c-\mu^2}\left[\frac{q_\rho(\mu^2)}{q_\rho(t)}\right]\left[\frac{1+R_\rho^2 q_\rho^2(t)}{1+R_\rho^2 q_\rho^2(\mu^2)}\right]\left[\frac{1+R_p^2 q_p^2(t)}{1+R_p^2 q_p^2(\mu^2)}\right]$$

where

$$q_\rho(t) = \frac{1}{2\omega}\left\{\left[(\omega-\mu)^2 - t\right]\left[(\omega+\mu)^2 - t\right]\right\}^{\frac{1}{2}}$$

and

$$q_p(t) = \frac{1}{2m_p}\left\{\left[4m_p^2 - t\right](-t)\right\}^{\frac{1}{2}}$$

are the momenta. The first factor is one introduced by Wolf[4] where $c=2.29\ \text{GeV}^2$. The second and third factors come from the ρ vertex. The fourth factor comes from the proton vertex. For R_p and R_ρ, the values used were

$$R_p = 2.86\ \text{GeV}^{-1}$$

$$R_\rho = 2.31\ \text{GeV}^{-1}$$

Since $q_p(t) \sim t$, the factor from the proton vertex becomes sizable even for small t. This will be seen in the conclusions.

III. Survey of Recent Literature in $\pi\pi$ and $K\pi$ Scattering

Many people have studied the $\pi\pi$ and $K\pi$ interactions. Some of the recent inquiries are discussed here.

Laurens[5] described a method of extrapolation with complex transformation. This method is based on the work of Ciulli[6] and Cutkosky and Deo.[7] When various approximations are made, this method amounts to defining the variable x as a function of momentum transfer:

$$X(\Delta^2) = \frac{\alpha\Delta^2 + \beta}{\Delta^2 + \delta}$$

where α, β, and δ are parameters determined by the desire to transform the physical region into the region -1, + 1. Since there is a

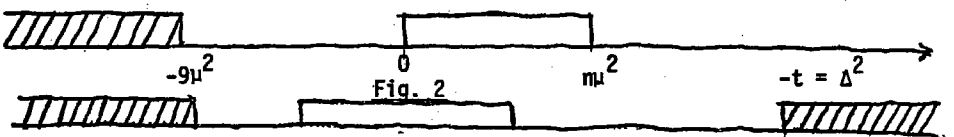

Fig. 2

Fig. 3

branch cut at $t=(3\mu)^2$ it is seen that the boundary conditions are

$$x(0) = -1$$

$$x(\mu^2) = +1$$

$$x(-\infty) = x(\infty) = \alpha$$

$$x(-9\mu^2) = -\alpha$$

where the physical region used is that for which $\Delta^2 < n\mu^2$. Then the parameters turn out to be

$$\delta = -\beta = 3(3 + \sqrt{9+n})\,\mu^2$$

$$\alpha = \frac{n+18}{n} + \sqrt{\left(\frac{n+18}{n}\right)^2 - 1}$$

Then the extrapolation is carried out in x rather than Δ^2. This x-extrapolation was used on the data in the present experiment. It gave, however,

results which were not significantly different from the original Chew-Low method.

Several people have used the x-extrapolation. Baillon[8] uses it in the measurement of the $\pi^+\pi^-$ cross section. He shows the angular distribution and δ . Jacques et al.[9] give preliminary results of Chew-Low extrapolations using $\pi^-p \to \pi^-\pi^+n$ at 4.5 GeV/c. They give a summary of different kinds of extrapolations for the total cross section including the x-extrapolation, Durr-Pilkuhn extrapolation and ordinary Chew-Low extrapolation.

A number of people have worked on $\pi\pi$ phase shifts. Villet et al.[10] do a $\pi\pi$ phase shift analysis from an experiment $\pi^-p \to \pi^o\pi^on$ at 2 GeV/c supplemented by $\pi^+\pi^-$, $\pi^-\pi^o$, $\pi^+\pi^+$ final states. They use Chew-Low extrapolation to do the $\pi\pi$ phase shift analysis. They find large J=0 production approaching the unitary limit in the 450-750 MeV $\pi\pi$ mass for $\pi^+\pi^- \to \pi^o\pi^o$. Scattering lengths are calculated as well as phase shifts. Another study of $\pi\pi$ phase shifts is done by Toaff et al.[11] in the energy region 0.6 to 1.42 GeV. The reaction $\pi^+n \to \pi^+\pi^-p$ is examined at 6 GeV/c. The phase shifts η_2^o, η_o^o, and δ are extracted. Also $d\alpha/dt$, $\cos\theta$, and Trieman-Yang angle distributions are shown for ρ^o and f. Grayer et al.[12] study isospin 2 $\pi\pi$ phase shifts from an experiment $\pi^+p \to \pi^+\pi^+n$ at 12.5 GeV/c. Moments are calculated for the I=2 $\pi\pi$ case. Also the phase shifts δ_s^2 and δ_d^2 are calculated. In addition Beier[13] has studied Ke4 and low energy $\pi\pi$ shifts. He looks at the decay $K_{e4}^{\pm} \to \pi^+\pi^-e^{\pm}\nu$. Low energy phase shifts are calculated and compared with data at higher $\pi\pi$ mass. Also $< \delta_s - \delta_s >$ is calculated and found to be $.19 \pm .05$. He shows that the low energy pion-pion interaction is weak and that the energy dependence of the phase shift is significant.

Several people have studied $\pi\pi$ phase shifts in connection with amplitude zeros. Hyams et al,[14] Manner[15], and Pennington.[16]

Estabrooks et al.[17] do a complete $\pi\pi$ phase shift analysis by a method based on an amplitude analysis of the production process and the extrapolation of the dominant π exchange amplitudes to the π exchange pole. A number of Argand diagrams are shown. The analysis is energy independent. Charlesworth et al.[18] study production of ρ^o and f^o in 4 GeV/c $\pi^+ d$ interactions. They apply the Estabrooks and Martin analysis[17] to the reaction $\pi^+ n \to p\rho^o$. Also the f^o is investigated. In addition Estabrooks and Martin[19] discuss $\pi^- p \to \pi^-\pi^+ n$ amplitude analysis and extrapolaiion to the π exchange pole. They solve analytically for the ampltides in the reaction $\pi^- p \to \pi^-\pi^+ n$ in the ρ region. They discuss the extrapolation of s-channel and t-channel ampltidues to the π pole and conclude that the s-channel extrapolation should be used for $\pi\pi$ phase shift analyses.

Coupled channels; Williams[20] does a theoretical study of $\pi\pi$ coupled channels, particulary the $\pi\pi \to K\bar{K}$ channel. He also discusses how to extract the $\pi\pi$ total cross section from the reaction $\pi^+ p \to \Delta^{++}$ + anything. In addition Grayer et al.[21] do a coupled channel analysis in the $K\bar{K}$ threshold region. The reaction $\pi \pm p \to \pi \pm \pi^+ n$ and $\pi^- p \to K^+K^- n$ are investigated. An energy-dependent phase shift analysis is done. Cross sections and moments are extrapolated for the reaction $\pi^+\pi^- \to K^+K^-$.

IV. Experiment

A. General

The present experiment was performed at the Berkeley Bevatron. The 25" bubble chamber was used as a detector. 300,000 pictures were taken of $\pi^+ p$ interactions at a momentum of 2.67 BeV/c. These 300,000 pictures produced 90,000 two-prong events. Each of the pictures was taken in three views in order that a three dimensional reconstruction of the tracks could be made.

Two spectrometers and a number of quadrupoles were used to separate a beam of π^+ mesons at 2.67 BeV/c. A beam destroyer was used to deflect the proton beam from the target after ten π^+ mesons had gone through the bubble chamber. In this way the pictures uniformly had approximately ten incoming tracks per picture.

B. Scanning and Measuring

The pictures were scanned by scanners on roadmakers for two-prong events. In this process the positions of several fiducials, reference marks in the bubble chamber, and the event vertex are measured for each event and read into the computer. In addition points are taken along each of the three tracks that go into the vertex of the event. This information also goes into the computer.

The computer tape from the road makers is then read into the Flying Spot Digitizer (FSD). The FSD looks at the pictures with events and scans them in a manner similar to a TV camera, in two orthogonal directions.

When a scan hits a bubble on one of the tracks of an event, the FSD records a hit. When a scan passes between two bubbles, no hit is recorded. In this manner not only are the positions of the tracks recorded, but also information is obtained regarding the density of bubbles along the track, i.e., the amount of ionization along each track. Information on the ionization is helpful in determining the mass of each particle.

Information from the FSD is then read into the data reduction system FOG-CLOUDY-FAIR. In FOG the events are reconstructed in three dimensions. In CLOUDY myriads of quantities concerning the events are calculated. In FAIR a list of these quantities specified by the physicist are abstracted from the CLOUDY library. Then histograms, scatter plots, lists, or tapes as specified by the physicist can be done by FAIR.

C. Beam Normalization

Ko, working with the same film found a path length of $(4.314 \pm .130) \frac{\text{events}}{\mu b}$. The fiducial volume used by Ko was somewhat different from that used in this experiment. Hence a correction must be made. By looking at the number of events in Ko's fiducial volume versus the number of events in the fiducial volume of the present experiment, one can determine the correction factor. For a certain segment of the film there are 34,333 two-prong events in Ko's fiducial volume and 27,345 events in the fiducial volume of the present experiment. This leads to a correction factor of 27,345/34,333 = .7965. Hence the path length for this experiment is

$$(4.314 \pm .130) \frac{\text{events}}{\mu b} \times .7965 = (3.436 \pm .100) \frac{\text{events.}}{\mu b}$$

D. Experimental Efficiencies

The total number of events scanned at 2.67 BeV/c, excluding remeasures, was 85,716. The total number that came out from FAIR was 83,682. This gives a FAIR efficiency of

$$\varepsilon_f = 83{,}682/85{,}716 = .9763$$

The scanning efficiency was found to be $\varepsilon_s = .92$.

In addition cuts were made on TDAV, rms deviation of the measured points from the fitted curve, ITER; the number of iterations needed for convergence. These cuts eliminated 1100 events out of 27,345. Hence the cut efficiency is

$$\varepsilon_c = 1 - \frac{1100}{27{,}345} = .9598$$

The total efficiency is

$$\varepsilon = \varepsilon_f \varepsilon_s \varepsilon_c = .9763 \times .92 \times .9538 = .8621$$

Hence the effective path length is

$$L = (3.436 \pm .100) \times .8621 \ \frac{\text{events}}{\mu b}$$

$$= (2.962 \pm .076) \text{ events}/\mu b$$

This gives a microbarn equivalent of .34 μb/event.

E. Separation of Events

In the FOG-CLOUDY-FAIR system, events are fit to several different types

$$\pi^+ p \rightarrow \pi^+ p$$

$$\pi^+ p \rightarrow p\pi^+$$

$$\pi^+ p \rightarrow \pi^+ p\pi^o$$

$$\pi^+ p \rightarrow p\pi^+\pi^o$$

$$\pi^+ p \rightarrow \pi^+\pi^+ n$$

The events are fit after an examination of the energy-momentum relations.

Many events fit more than one type. Then the problem becomes one of separating these ambiguous events into their proper type.

Two χ^2's are calculated for each event and for each type that it fits. M * is the χ^2 for the fit to the energy-momentum relations. G*** is the χ^2 for the bubble density - for the way in which the bubble density balances the expected momentum of each track.

A quantity MG* was formed for each event and each type in the following manner. The distribution of each χ^2 was compared to the ideal χ^2 distribution known from statistics.

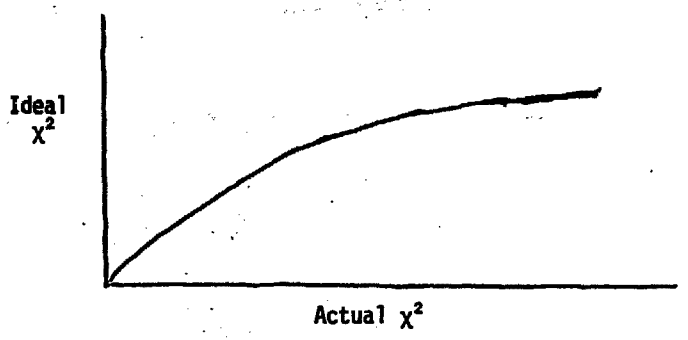

Fig. 4

The resulting curve was fit to a conic section with the following two stipulations:

(a) The curve must go through the point (0,0).

(b) At the point (0,0), the first derivative of the curve must be 1.

The curves therefore, were fit according to the following parameterization.

$$F(M^*, P_M, q_M, R_M) = [\sqrt{q_M^2 + 2q_M(M^*) + P_M(M^*)^2} - q_M]R_M$$

$$F(G^{***}, P_G, q_G, R_G) = [\sqrt{q_G^2 + 2q_G(G^{***}) + P_G(G^{***})^2} - q_G]R_G$$

The following values were found for q, P, and R:

$q_G = 10.0$

$P_G = 0.4$

$R_G = 1.0$

$q_M = 4.1$

$P_M = -.09$

$R_M = \begin{matrix} 1.4 \text{ for elastics} \\ 0.75 \text{ for non-elastics} \end{matrix}$

Then MG^* is formed:

$MG^* = F(M^*, P_M, q_M, R_M) + F(G^{***}, P_G, q_G, R_G)$. Since $F(M^*)$ has one degree of freedom and $F(G^{***})$ has 3 d.f., then MG^* is an ideal χ^2 variable with 4 d.f.

Then the ambiguous events are separated by choosing the type with the smallest MG^*.

One further problem needs to be dealt with. Some of the two-prong events have more than one neutral particle:

$$\pi^+ p \to \pi^+ p\, \pi^o \pi^o$$

$$\pi^+ p \to p \pi^+ \pi^o \pi^o$$

$$\pi^+ p \to \pi^+ \pi^+ n\, \pi^o$$

Hence one looks at the missing mass squared (M^2_m) for the type whose fit has the smallest G^{***}. If M^2_m is more than one standard deviation above the M^2 for a single neutral particle and also greater than the M^2 for two neutral particles at rest, then the event is assumed to have more than one neutral particle in it.

One can see how clean the sample is by looking at the Dalitz plot and Chew-Low plots. Fig. 5 shows the Dalitz plot. It also shows the projections

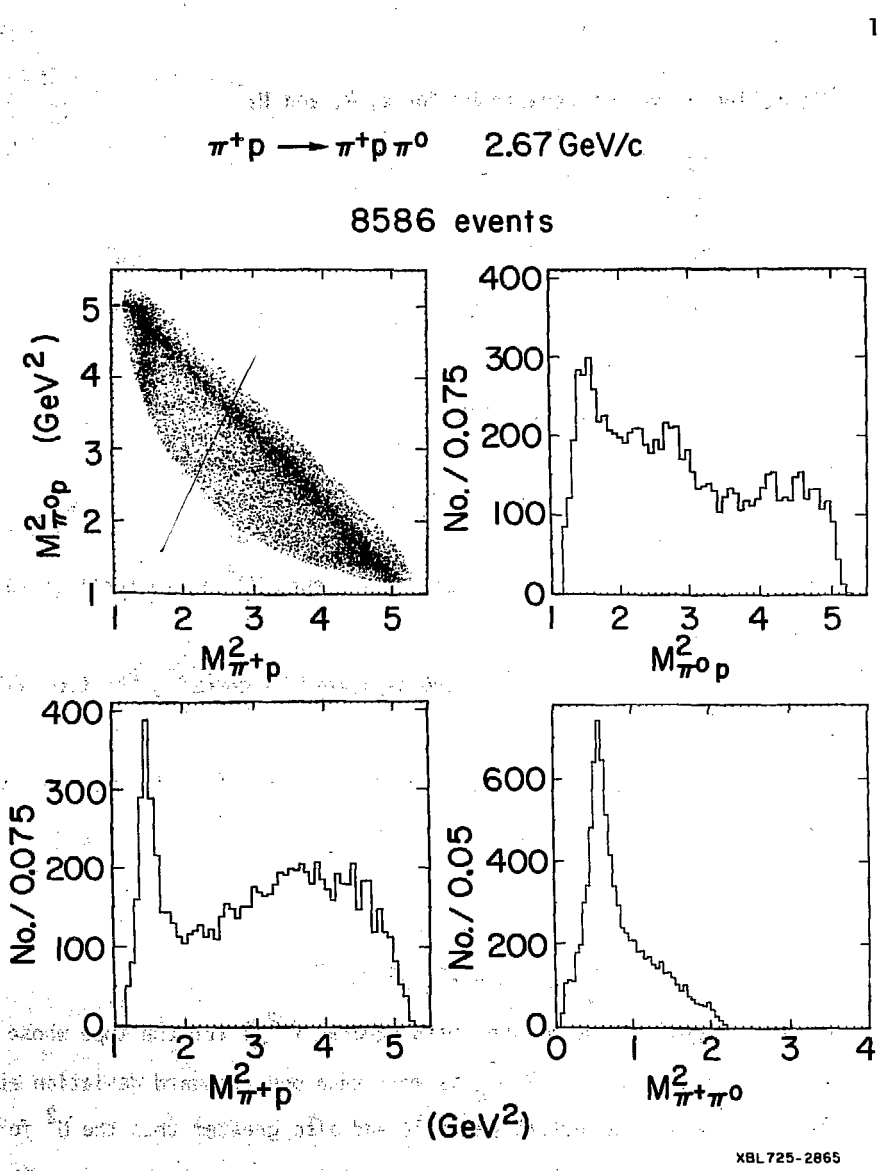
$\pi^+ p \longrightarrow \pi^+ p \pi^0$ 2.67 GeV/c
8586 events
$M^2_{\pi^0 p}$ (GeV^2)
$M^2_{\pi^+ p}$
No./0.075
$M^2_{\pi^0 p}$
No./0.075
$M^2_{\pi^+ p}$
No./0.05
$M^2_{\pi^+ \pi^0}$
(GeV^2)
XBL725-2865

Figure 5

on the three two-body mass systems. We see that the Dalitz plot is dominated by ρ^+ production. We also see the two Δ bands (Δ^+ and Δ^{++}) that provide some contamination but not too much. Figure 6 shows the three Chew-Low plots for the three different two-body mass systems. Figure 7 shows the Chew-Low plot for the $\pi^+\pi^o$ mass system with a projection on the -t axis. We see the dip at t=-0.5 due to Regge effects described by Gidal et al.[22] and others.

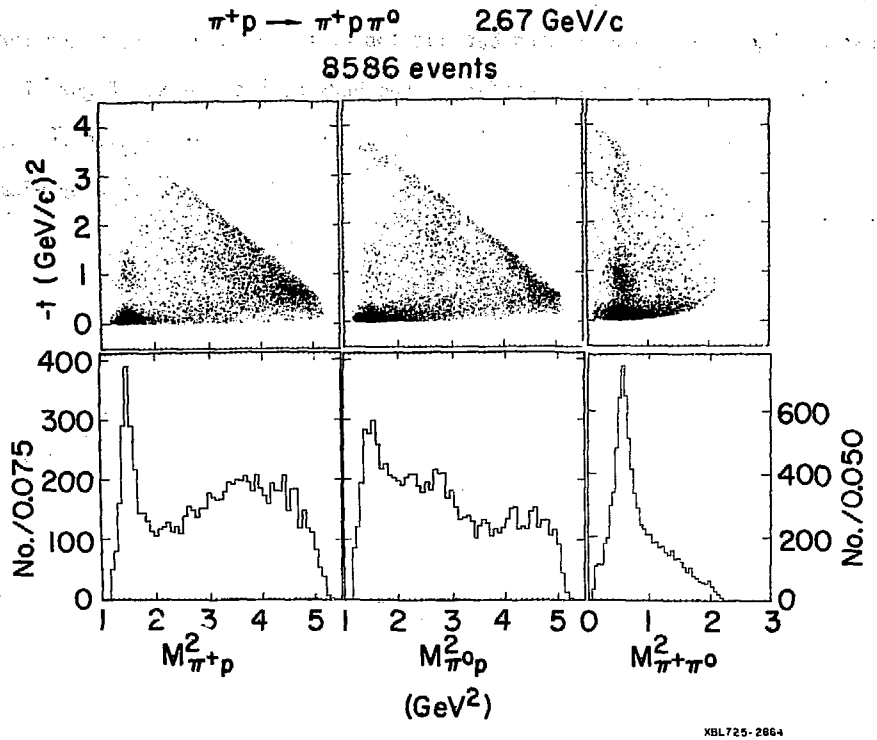
π+p — π+pπ0 2.67 GeV/c
8586 events
-t (GeV/c)2
No./0.075
No./0.050
M2π+p
M2π0p
M2π+π0
(GeV2)
XBL725-2864

Figure 6

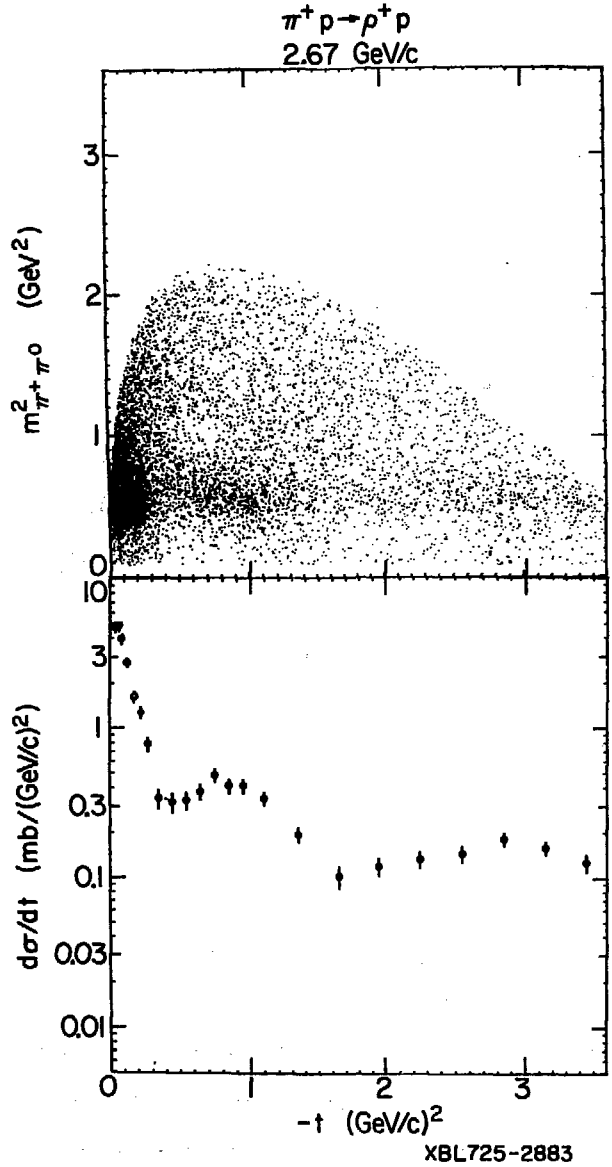
$\pi^+ p \to \rho^+ p$
2.67 GeV/c
$m^2_{\pi^+\pi^0}$ (GeV^2)
3
2
1
0
10
3
1
0.3
0.1
0.03
0.01
$d\sigma/dt$ (mb/(GeV/c)^2)
0
1
2
3
$-t$ (GeV/c)^2
XBL725-2883

Figure 7

V. Results and Conslusions

A. The Data Sample

The final data sample consists of 13,066 events of the reaction $\pi^+p \to \pi^+p\pi^o$ and 6232 events of the reaction $\pi^+p \to \pi^+\pi^+n$.

The Dalitz plot of the reaction $\pi^+p \to \pi^+\pi^+n$ is shown in Fig. 8. It is flat, but one can see an enhancement in π^+n at a mass^2 of about 2.8. This shows up as a cross in Fig. 8. The two projections on mass^2 of this Dalitz plot are shown in Fig. 9.

Figure 10 shows $\cos\theta_{cm}$ for events in the ρ band. This is essentially the t distribution. We see that the distribution is very forwardly peaked. Figure 11 shows the t dependence for four bands of mass^2 $(\pi^+\pi^o)$ in the region $-t \leq .238 = 13\mu^2$. This t cut is the one used in this experiment. The t was chosen small enough to suppress extraneous processes and yet large enough to give sufficient lever arm to carry out the extrapolation.

Figure 12 shows the distribution of mass^2 (π^+p) for events in the ρ band and somewhat above. One can see the large amount of Δ^{++} in the sample. Is this something to be concerned about? In Figure 13 the Dalitz plot is shown for those events with $-t \leq .238 = 13\mu^2$. The events at high mass^2 $(\pi^+\pi^o)$ are eliminated by the t cut. Figure 14a gives the mass^2 (π^+p) distribution for the events with the t cut and $.45 <$ mass^2 $(\pi^+\pi^o) < 1.00$. In Figures 14b, 14c,14d are shown the same distribution for three t regions within this t cut. It is apparent that, as t approaches the pole, the distribution approaches more and more the $\cos^2\theta$ distribution of the ρ. Hence we conclude that the Δ contamination is not a problem as one goes to the pole.

The distribution in mass^2 $(\pi^+\pi^o)$ of the events with the t cut is shown in Fig. 15. These are the events with which this experiment will be concerned. The large ρ peak is apparent.

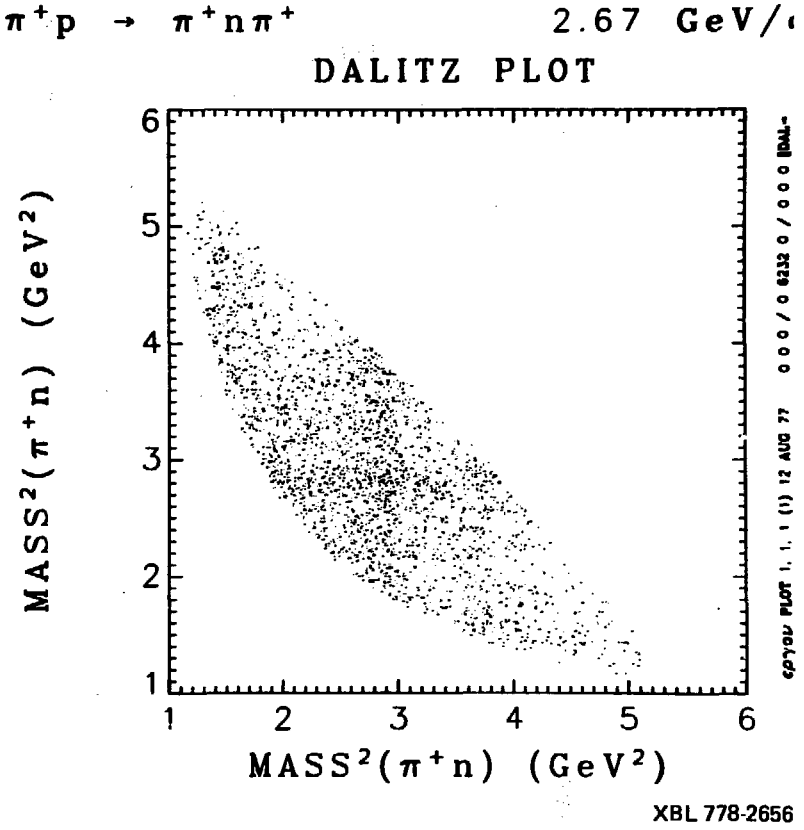
π⁺p → π⁺nπ⁺ 2.67 GeV/
DALITZ PLOT
MASS²(π⁺n) (GeV²)
MASS²(π⁺n) (GeV²)
1
2
3
4
5
6
XBL 778-2656

Figure 8

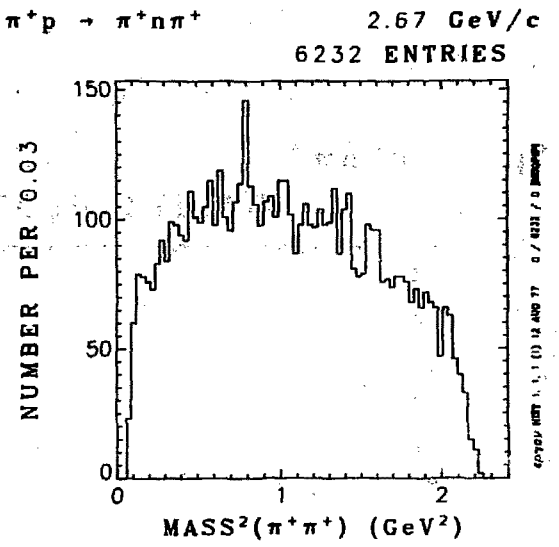

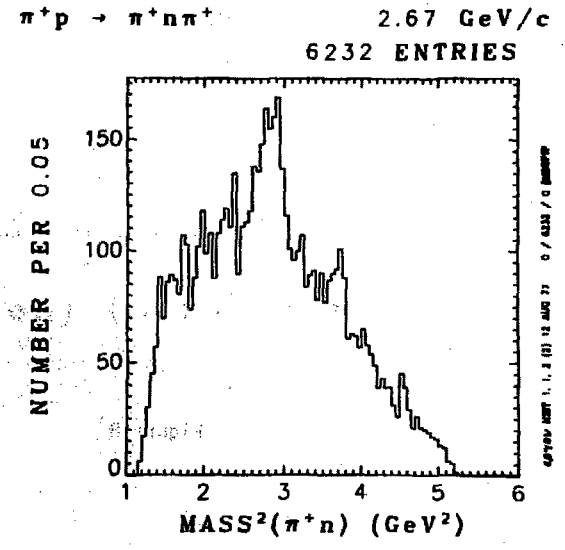

XBL 778-2715

Figure 9

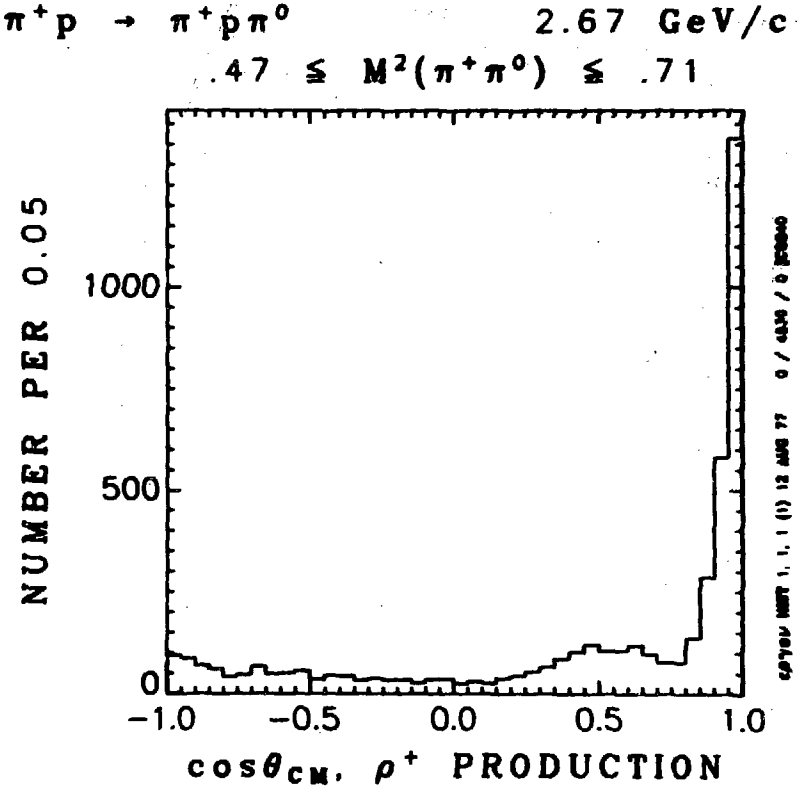

XBL 778-2667

Figure 10

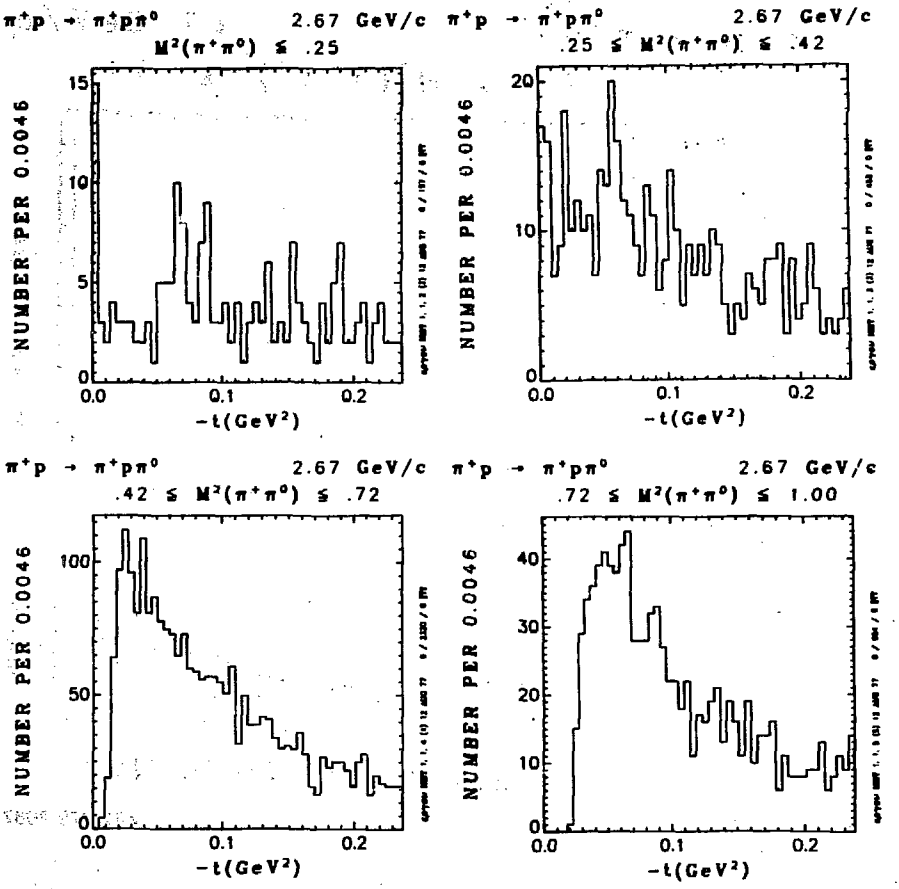
π⁺p → π⁺pπ⁰ 2.67 GeV/c
M²(π⁺π⁰) ≤ .25
.25 ≤ M²(π⁺π⁰) ≤ .42
.42 ≤ M²(π⁺π⁰) ≤ .72
.72 ≤ M²(π⁺π⁰) ≤ 1.00
NUMBER PER 0.0046
-t(GeV²)
XBL 778-2720

Figure 11

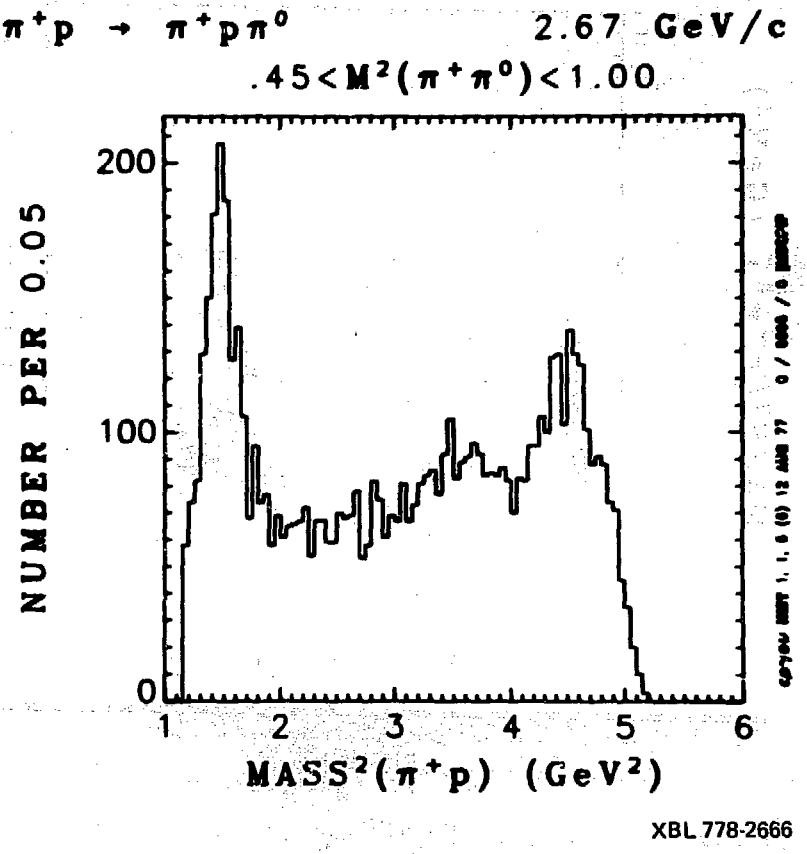
$\pi^+p \rightarrow \pi^+p\pi^0$
2.67 GeV/c
$.45 < M^2(\pi^+\pi^0) < 1.00$
NUMBER PER 0.05
200
100
0
1
2
3
4
5
6
$MASS^2(\pi^+p)$ (GeV^2)
XBL 778-2666

Figure 12

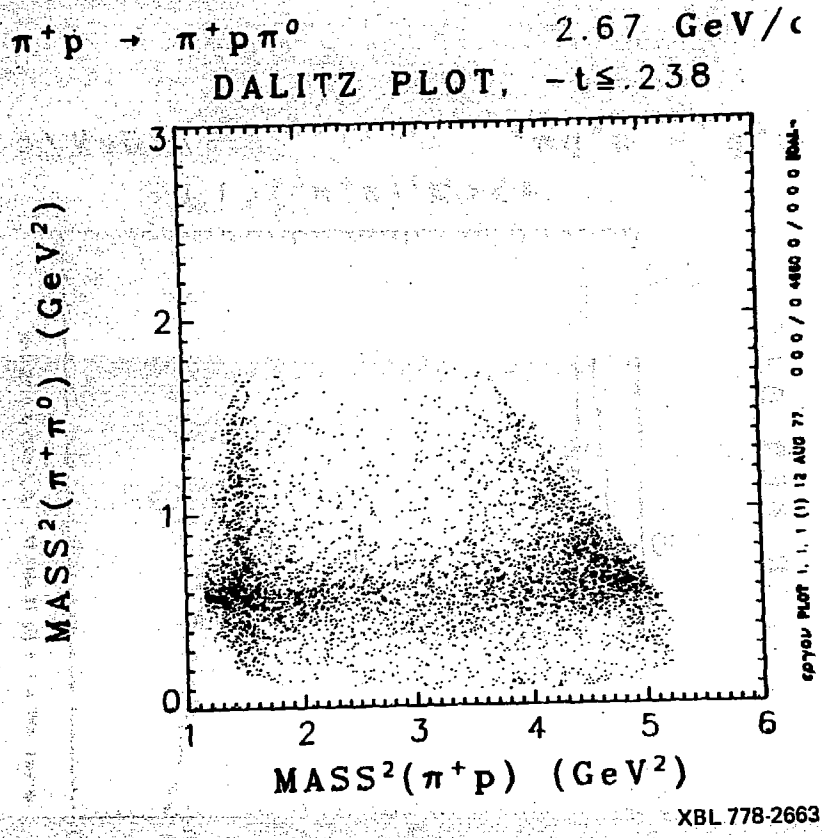

XBL 778-2663

Figure 13

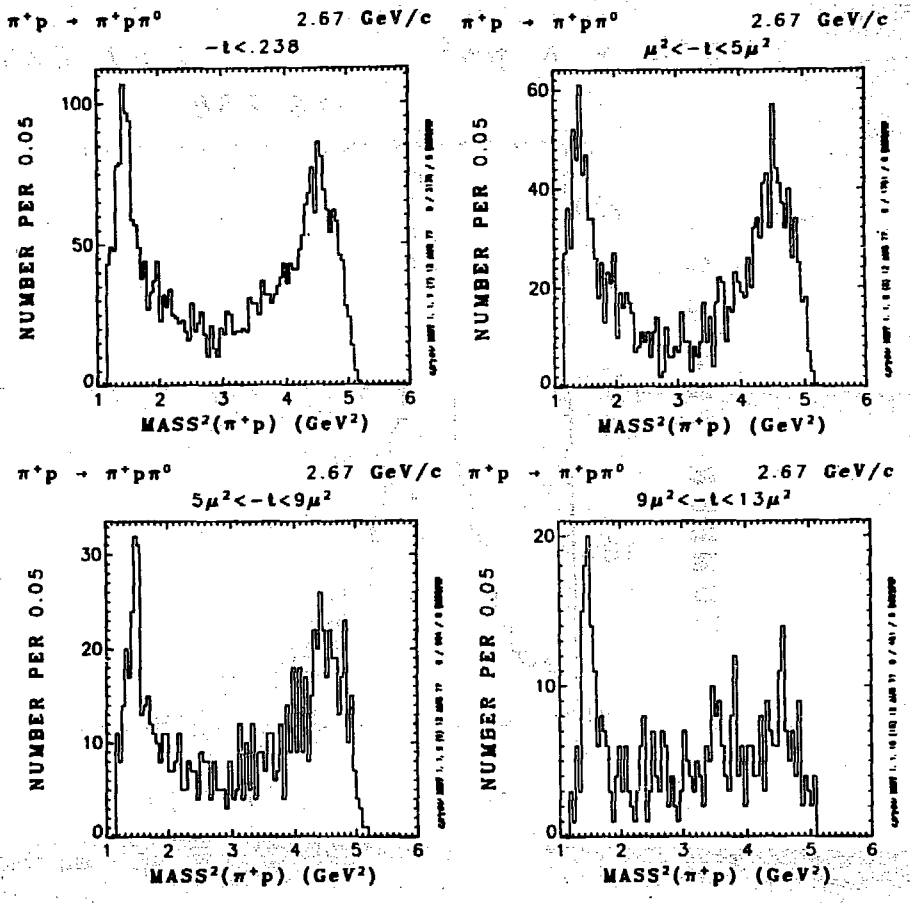
π⁺p → π⁺pπ⁰ 2.67 GeV/c
−t<.238
NUMBER PER 0.05
MASS²(π⁺p) (GeV²)
π⁺p → π⁺pπ⁰ 2.67 GeV/c
μ²<−t<5μ²
NUMBER PER 0.05
MASS²(π⁺p) (GeV²)
π⁺p → π⁺pπ⁰ 2.67 GeV/c
5μ²<−t<9μ²
NUMBER PER 0.05
MASS²(π⁺p) (GeV²)
π⁺p → π⁺pπ⁰ 2.67 GeV/c
9μ²<−t<13μ²
NUMBER PER 0.05
MASS²(π⁺p) (GeV²)
XBL 778-2719

Figure 14

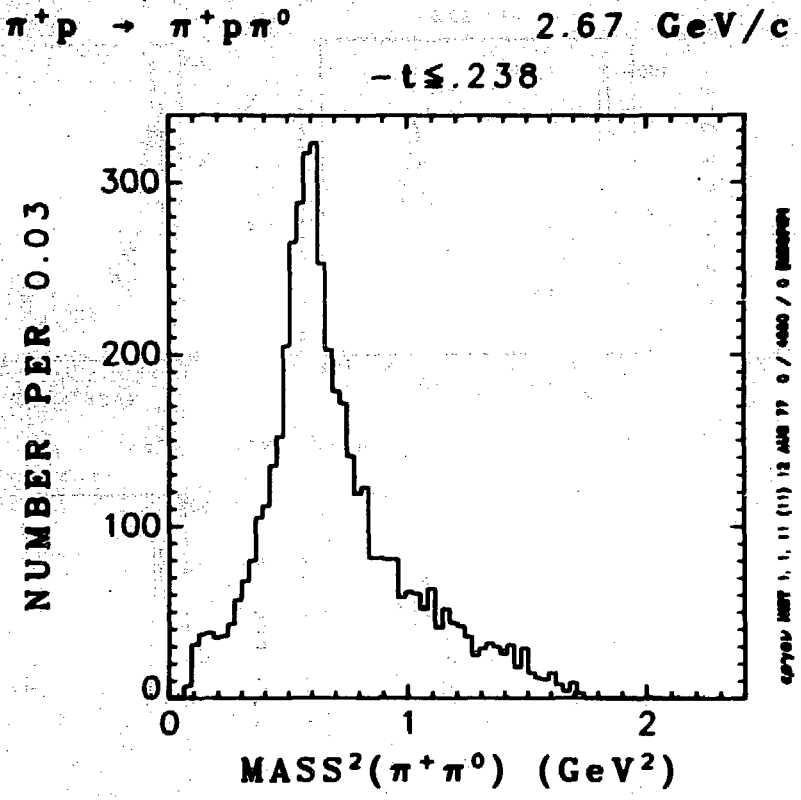

XBL 778-2665

Figure 15

The cos of the Jackson angle for four bands in mass^2 ($\pi^+\pi^o$) with the $\tilde{t}$ cut is shown in Fig. 16. In Fig. 16c we see the $\cos^2\theta$ dependence for the events in the ρ band. Figure 17a shows a plot of the Trieman-Yang angle versus cosθ Jackson for the ρ events. Figure 17b shows the same plot for the events that are also in the Δ^{++} band. The Δ events are clustered in one particular area of the plot.

Consider the reaction $\pi^+p \to \pi^+\pi^+n$. Figure 18 gives the distribution in $\cos\theta_{cm}$ for events with intermediate values of mass^2 ($\pi^+\pi^+$). The events are strongly peaked in the forward direction.

Figure 19 shows mass^2 ($\pi^+\pi^+$) for events with the $\tilde{t}$ cut. Here is the mass distribution of the events to be extrapolated. Figure 20 presents the cosθ Jackson distribution for four different bands in mass^2 ($\pi^+\pi^+$). There seems to be a $\cos^2\theta$ component in the upper two bands. Figure 21 gives the $\tilde{t}$ distribution for events in the same four bands of mass^2 ($\pi^+\pi^+$). These histograms show the events to be extrapolated.

Figure 22 shows a Dalitz plot for the events with the $\tilde{t}$ cut. The events with high mass ($\pi^+\pi^+$) have been eliminated. In Fig. 23 there is a Chew-Low plot for all $\pi^+\pi^+n$ events. Most of the events are clustered at low values of $|\tilde{t}|$.

B. Experimental Calculations

For the reaction $\pi^+p \to \pi^+p\pi^o$ there were 2893 events with momentum transfer between μ^2 and $13\mu^2$($\mu^2 \leq -t \leq 13\mu^2$) and $\pi\pi$ mass between 280 MeV and 1050 MeV. The extrapolations were made according to both the Chew-Low method and the Durr-Pilkuhn method. In the Chew-Low method it is assumed that the data in the physical region ($-t > 0$) fit a straight line ($a+b(-t)$) and the limit is taken by extrapolating this straight line to the point $t=\mu^2(\sigma_{\pi\pi} = a-b\mu^2)$. The parameters a and b are determined by finding those

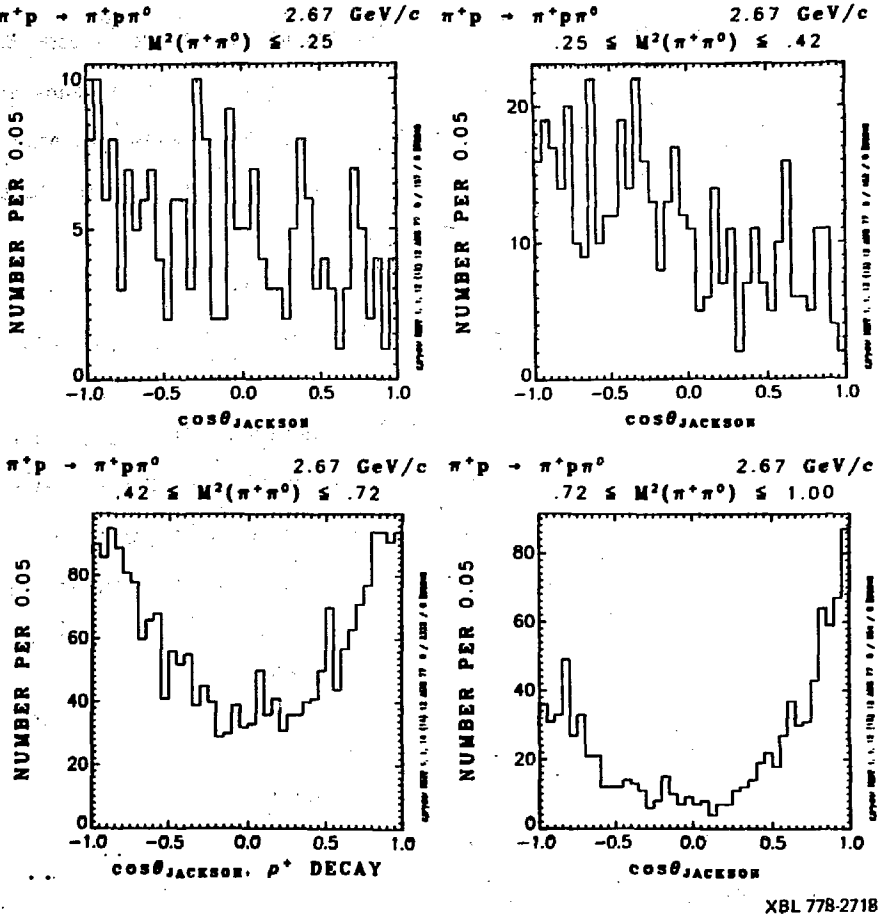

XBL 778-2718

Figure 16

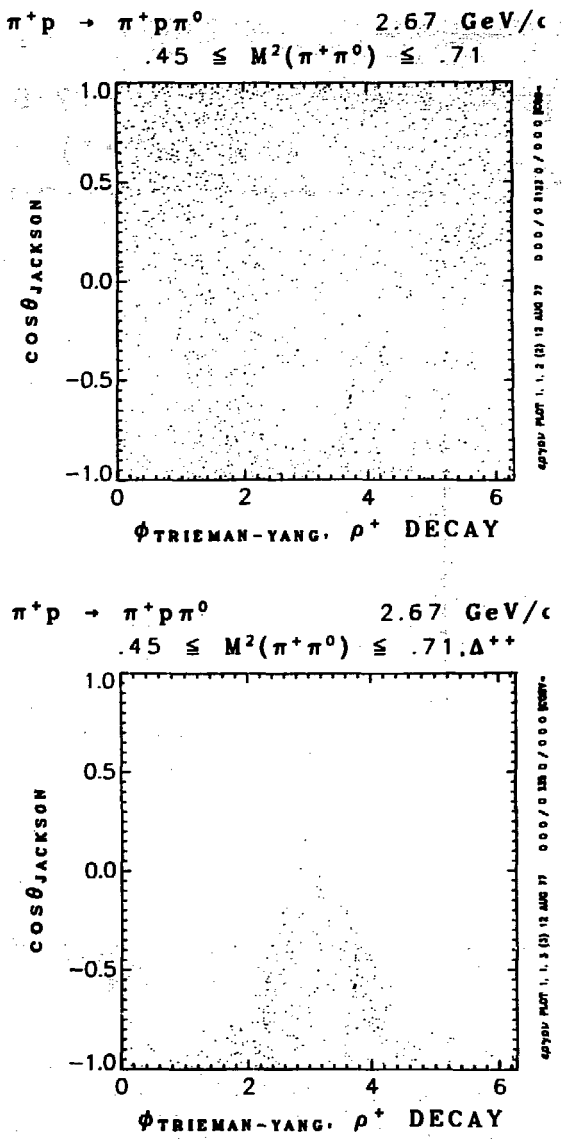

XBL 778-2714

Figure 17

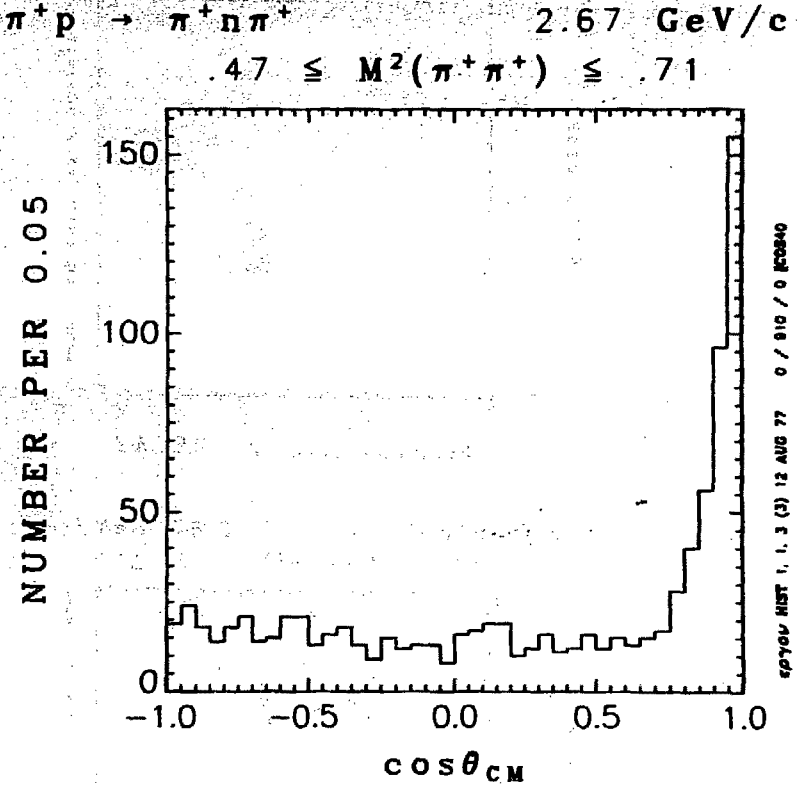

XBL 778-2661

Figure 18

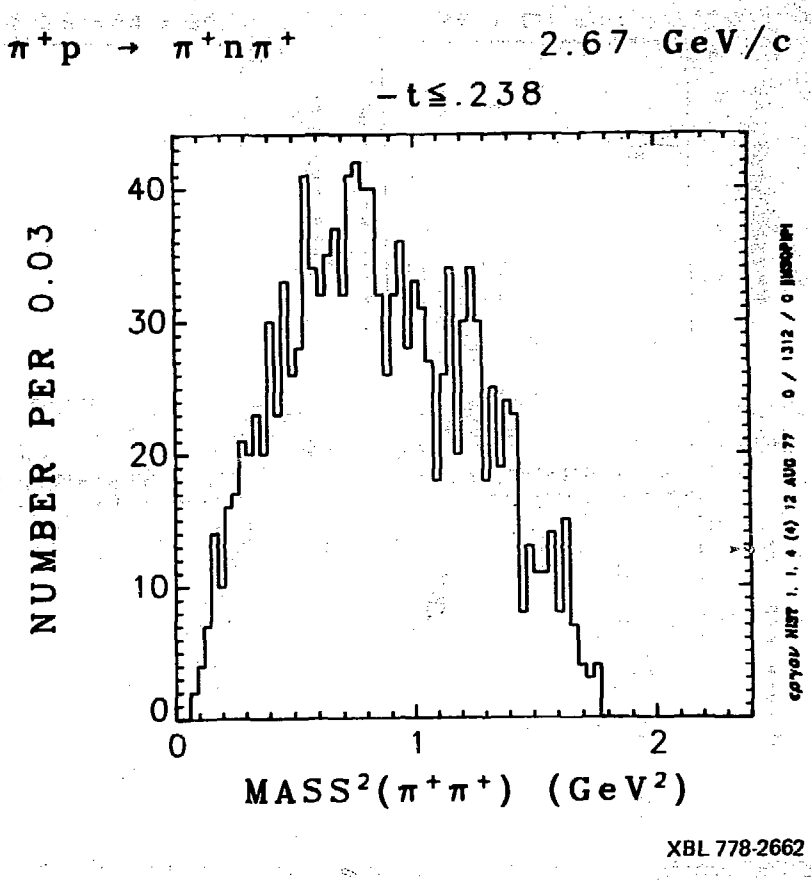
$\pi^+ p \rightarrow \pi^+ n \pi^+$
2.67 GeV/c
$-t \leq .238$
NUMBER PER 0.03
40
30
20
10
0
0
1
2
MASS$^2(\pi^+\pi^+)$ (GeV^2)
XBL 778-2662

Figure 19

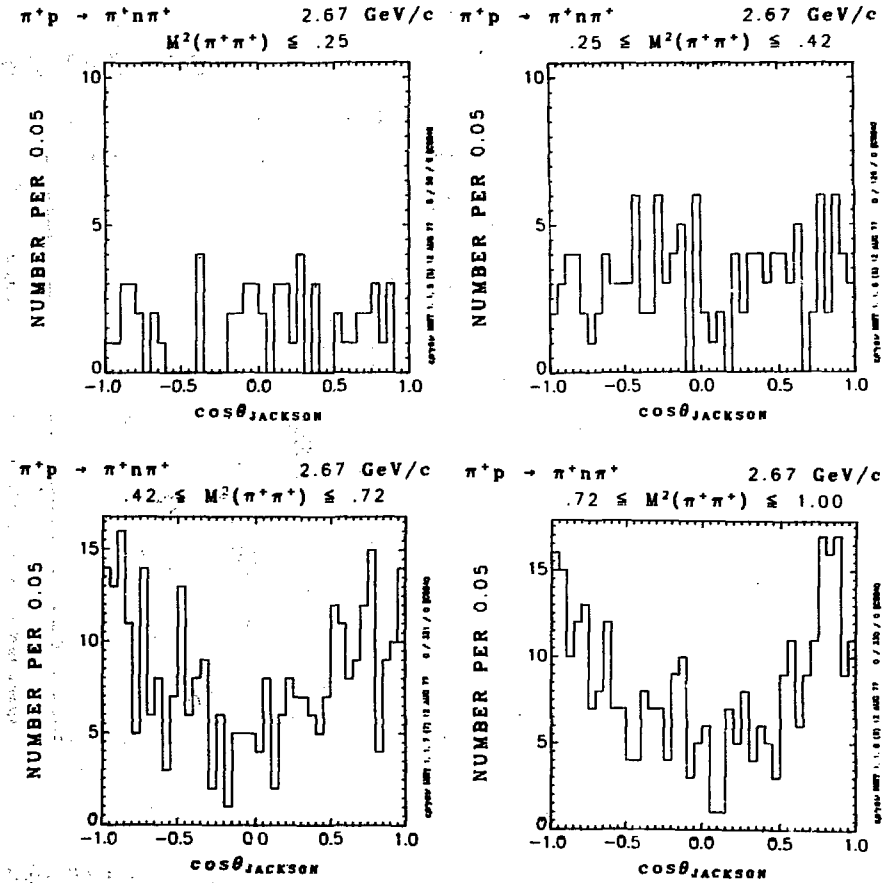
π⁺p → π⁺nπ⁺ 2.67 GeV/c
M²(π⁺π⁺) ≤ .25
.25 ≤ M²(π⁺π⁺) ≤ .42
.42 ≤ M²(π⁺π⁺) ≤ .72
.72 ≤ M²(π⁺π⁺) ≤ 1.00
NUMBER PER 0.05
cosθJACKSON
XBL 778-2717

Figure 20

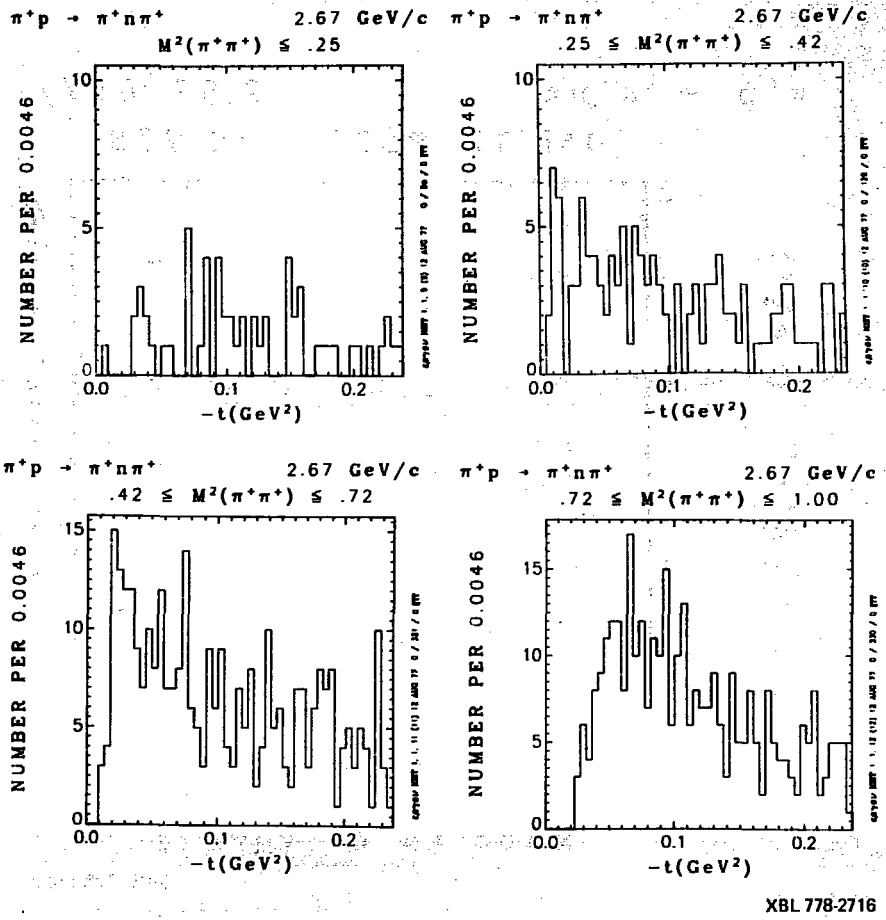
π⁺p → π⁺nπ⁺ 2.67 GeV/c
M²(π⁺π⁺) ≤ .25
.25 ≤ M²(π⁺π⁺) ≤ .42
.42 ≤ M²(π⁺π⁺) ≤ .72
.72 ≤ M²(π⁺π⁺) ≤ 1.00
NUMBER PER 0.0046
−t(GeV²)
0.0
0.1
0.2
0
5
10
15
XBL 778-2716

Figure 21

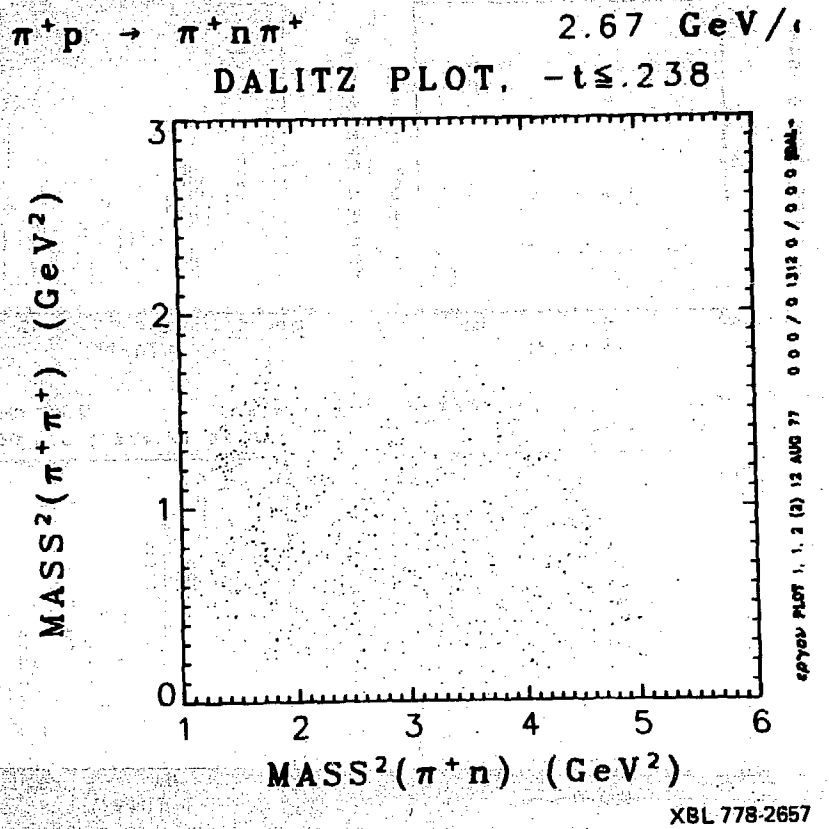
$\pi^+ p \rightarrow \pi^+ n \pi^+$
2.67 GeV/
DALITZ PLOT, $-t \leq .238$
$MASS^2(\pi^+\pi^+)$ (GeV^2)
$MASS^2(\pi^+ n)$ (GeV^2)
0
1
2
3
4
5
6
XBL 778-2657

Figure 22

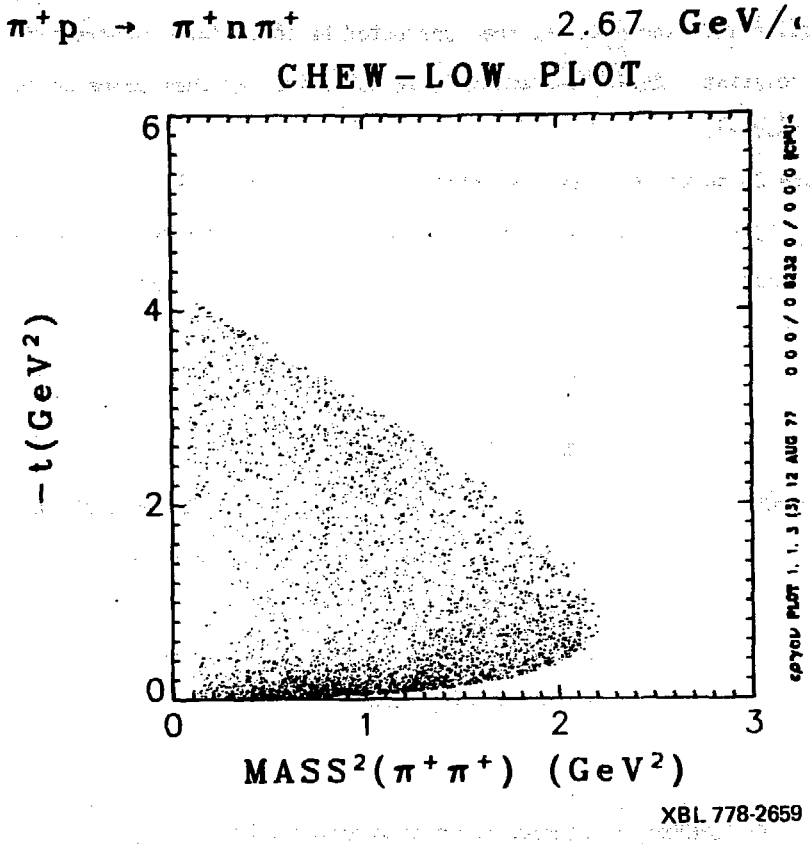
$\pi^+ p \rightarrow \pi^+ n \pi^+$ 2.67 GeV/
CHEW-LOW PLOT
$-t\,(GeV^2)$
$MASS^2(\pi^+\pi^+)$ (GeV^2)
0
1
2
3
4
6
XBL 778-2659

Figure 23

values which give minimum χ^2. In the Durr-Pilkuhn method it is assumed that the data follow a curve specified by the additional form factors referred to in Section II. The data are then corrected by these form factors and fit to a constant. Again, the constant is determined by that value which gives minimum χ^2.

Figure 24 shows the Chew-Low extrapolation of the total $\pi\pi$ cross section. Figure 25 shows the $\pi\pi$ cross section extrapolated by the Durr-Pilkuhn method. The results at the ρ meson peak differ by approximately a factor of two. This difference comes primarily from the factor

$$\frac{1 + R_p^2 a_p^2 (-t)}{1 + R_p^2 a_p^2 (-\mu^2)}$$

in the Durr-Pilkuhn form factors, since $a_p^2 (-t) \sim (-t)$. We see that in Figure 25 the ρ peak reaches the unitary limit as one would expect, since the branching ratio for $\rho \to \pi\pi$ is almost 100%. Whereas in Fig. 24 the peak is only half the unitary limit. Hence it appears that the Durr-Pilkuhn method gives a value for the $\pi\pi$ cross section that is closer to what we would expect.

In addition, one would like to know about the angular distribution. Hence the density matrix elements ρ_{00}, $\rho_{1,1} + \rho_{1,-1}$ and $\rho_{1,1} - \rho_{1,-1}$ were extrapolated. We know that $\rho_{00} \frac{d\sigma}{dt}$ gives us the unnatural parity spin non-flip component, $(\rho_{1,1} + \rho_{1,-1}) \frac{d\sigma}{dt}$ the natural parity spin flip component, and $(\rho_{1,1} - \rho_{1,-1}) \frac{d\sigma}{dt}$ the unnatural parity spin flip component. One would expect the reaction $\pi^+ + \pi^o \to \rho^+ \to \pi^+ + \pi^o$ to be all ρ_{00} since the pion has zero spin.

The extrapolated values of $\rho_{00} \frac{d\sigma}{dt}$, $(\rho_{1,1} + \rho_{1,-1}) \frac{d\sigma}{dt}$, and $(\rho_{1,1} - \rho_{1,-1}) \frac{d\sigma}{dt}$ are shown in Figures 26 and 27 according to both the Chew-Low and

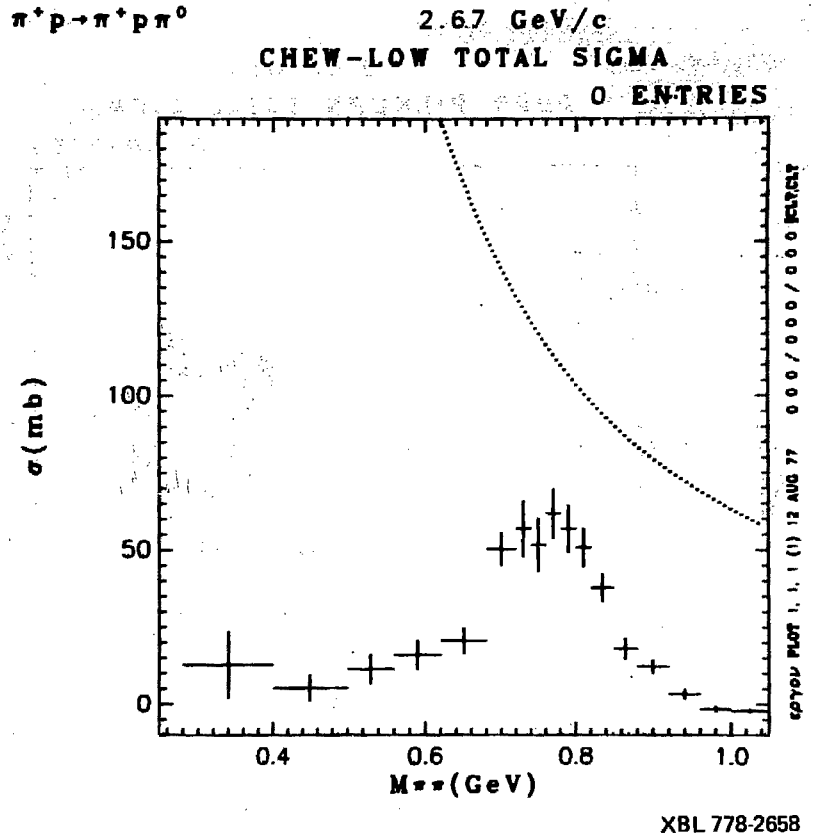
π⁺p→π⁺pπ⁰
2.67 GeV/c
CHEW-LOW TOTAL SIGMA
0 ENTRIES
σ(mb)
150
100
50
0
0.4
0.6
0.8
1.0
M**(GeV)
XBL 778-2658

Figure 24

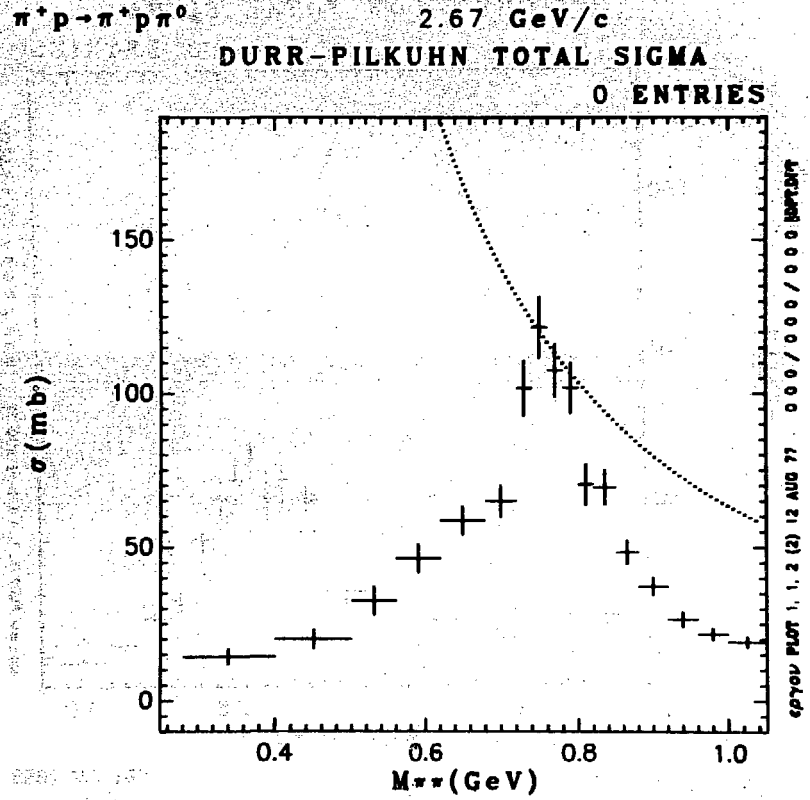

XBL 778-2660

Figure 25

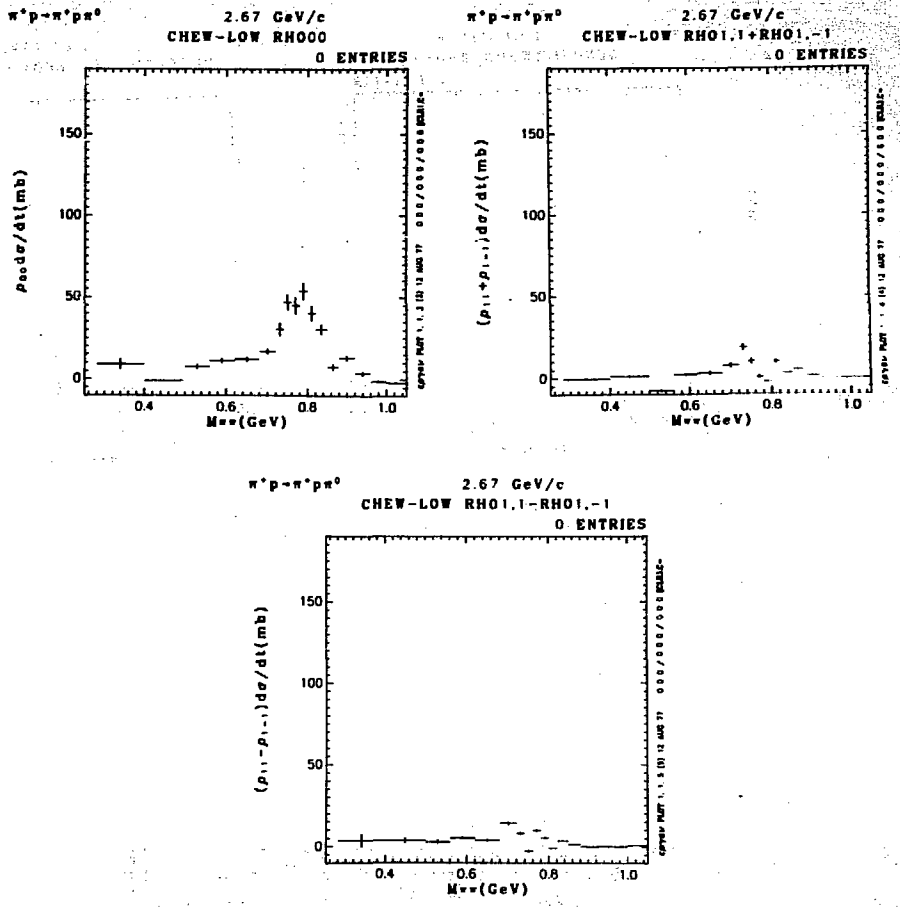
π⁺p→π⁺pπ⁰ 2.67 GeV/c
CHEW-LOW RHO00
0 ENTRIES
ρ₀₀dσ/dt(mb)
Mππ(GeV)
π⁺p→π⁺pπ⁰ 2.67 GeV/c
CHEW-LOW RHO1,1+RHO1,-1
0 ENTRIES
(ρ1,1+ρ1,-1)dσ/dt(mb)
Mππ(GeV)
π⁺p→π⁺pπ⁰ 2.67 GeV/c
CHEW-LOW RHO1,1-RHO1,-1
0 ENTRIES
(ρ1,1-ρ1,-1)dσ/dt(mb)
Mππ(GeV)
XBL 778-2713

Figure 26

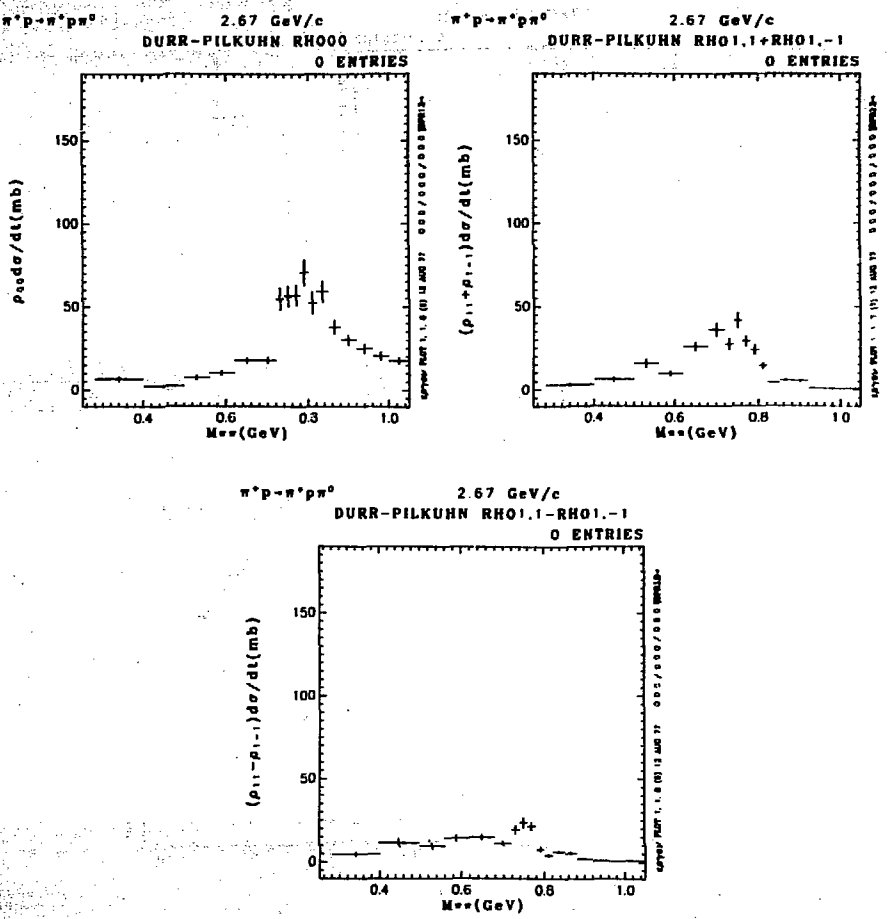

XBL 778-2712

Figure 27

Durr-Pilkuhn methods of extrapolation. These were found by extrapolating:

$$\rho_{00} \frac{d\sigma}{dt} = (1/2(5\overline{\cos^2\theta} - 1)) \frac{d\sigma}{dt}$$

$$(\rho_{1,1} + \rho_{1,-1}) \frac{d\sigma}{dt} = (1/4 (3-5(\overline{\cos^2\theta} + \overline{\sin^2\theta \cos^2\phi}))) \frac{d\sigma}{dt}$$

$$(\rho_{1,1} - \rho_{1,-1}) \frac{d\sigma}{dt} = (1/4(3-5(\overline{\cos^2\theta} - \overline{\sin^2\theta \cos^2\phi}))) \frac{d\sigma}{dt}$$

where θ and ϕ are the Jackson angle and the Trieman-Yang angle, respectively.

We see that the Chew-Low extrapolation shows practically all ρ_{00} and very little $\rho_{1,1} + \rho_{1,-1}$ and $\rho_{1,1} - \rho_{1,-1}$ as we would expect. On the other hand the Durr-Pilkuhn method shows considerable $\rho_{1,1} + \rho_{1,-1}$ and $\rho_{1,1} - \rho_{1,-1}$. So it would seen that the Chew-Low method is better than the Durr-Pilkuhn for extrapolating angular distributions. Perhaps there is some defect in the Durr-Pilkuhn method which renders it inapplicable to the extrapolation of angular distributions. Or perhaps our reaction $\pi^+ p \to \pi^+ p\pi^o$ takes place by something other than one pion exchange (OPE).

One thing that was considered was whether or not, some of the short protons were being missed in the first t bin ($\mu^2 \leq -t \leq 3\mu^2$). Hence a plot was made of the azimuthal angle of the proton in the first t bin. One can see from Figure 28 that the distribution is quite flat. Hence it is assumed that we are not missing many short protons.

In order to look for more information about the angular distribution, the spherical harmonics were examined. Histograms were made with the low $-t$ events weighted by the various spherical harmonics. These histograms are shown in Figure 29 for Y_{10}, Y_{11}, Y_{20}, Y_{21} and Y_{22}. One question was whether or not the Δ^{++} events were influencing the distributions. So the Δ events were removed and the same histograms plotted. These are shown in Figure 30. We see that they do not differ significantly from the previous

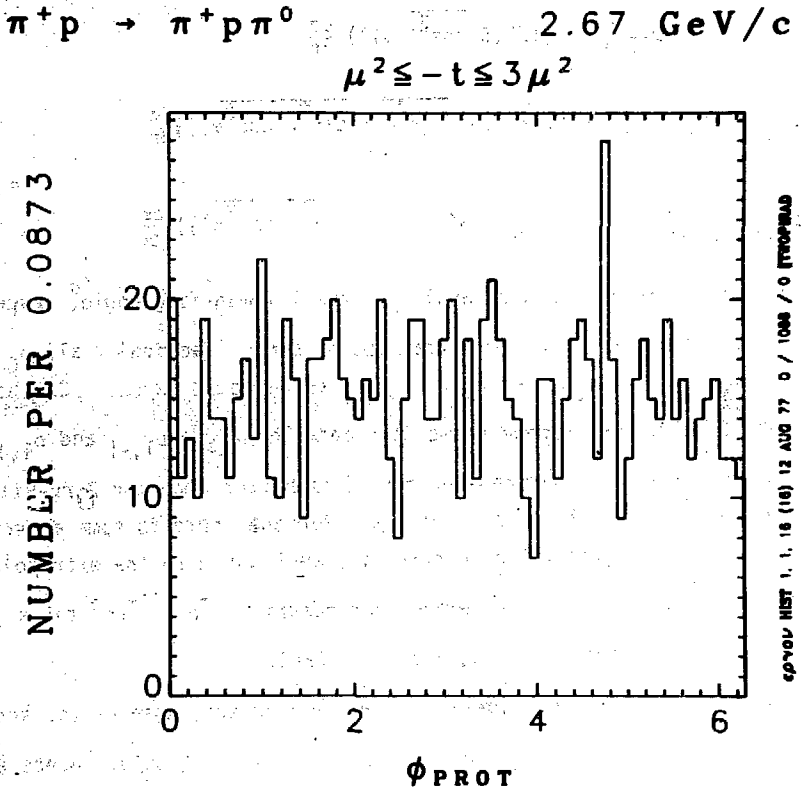

XBL 778-2664

Figure 28

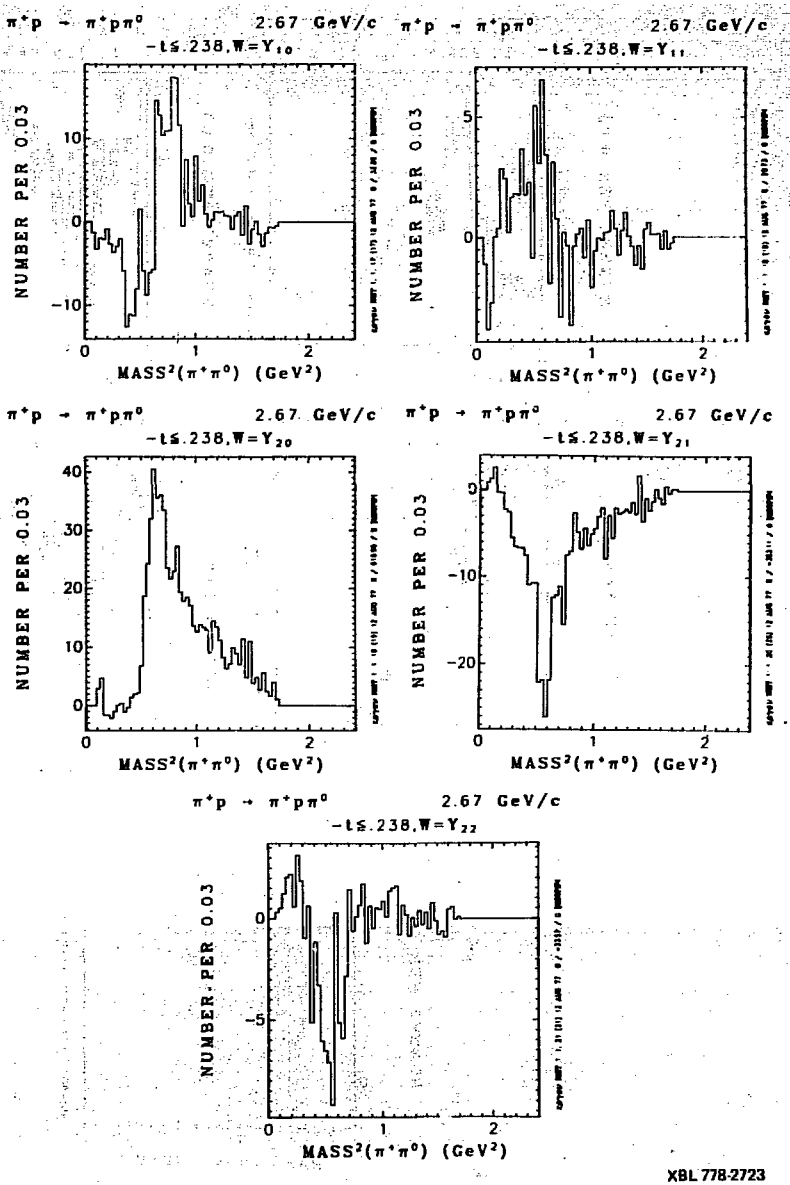

XBL 778-2723

Figure 29

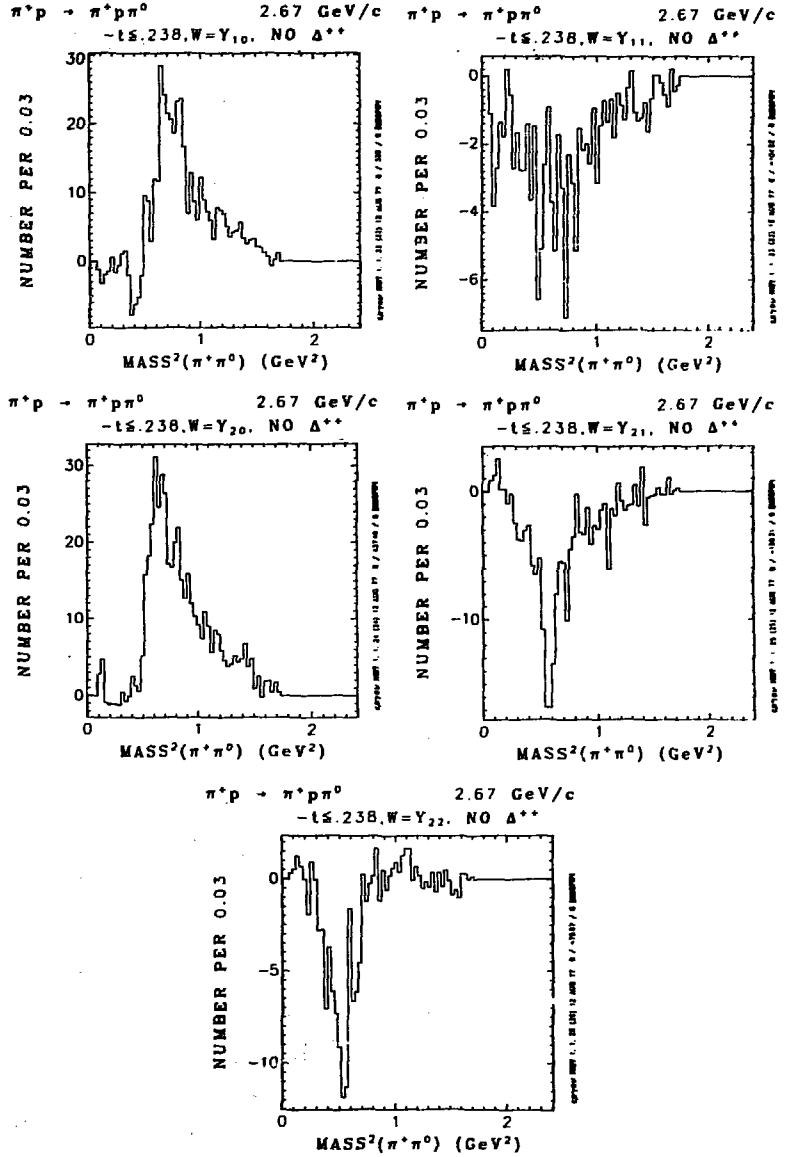
$\pi^+p \to \pi^+p\pi^0$ 2.67 GeV/c
$-t \leq .238, W = Y_{10}$, NO Δ^{++}
$\pi^+p \to \pi^+p\pi^0$ 2.67 GeV/c
$-t \leq .238, W = Y_{11}$, NO Δ^{++}
$\pi^+p \to \pi^+p\pi^0$ 2.67 GeV/c
$-t \leq .238, W = Y_{20}$, NO Δ^{++}
$\pi^+p \to \pi^+p\pi^0$ 2.67 GeV/c
$-t \leq .238, W = Y_{21}$, NO Δ^{++}
$\pi^+p \to \pi^+p\pi^0$ 2.67 GeV/c
$-t \leq .238, W = Y_{22}$, NO Δ^{++}
NUMBER PER 0.03
MASS$^2(\pi^+\pi^0)$ (GeV^2)
XBL 778-2722

Figure 30

five histograms. Hence it seems that the Δ events do not make that much of a difference.

The average values of the spherical harmonics Y_{00}, Y_{10}, Y_{11}, Y_{20}, Y_{21}, Y_{22}, and Y_{30} were extrapolated by both the Chew-Low method and the Durr-Pilkuhn method. In the Chew-Low method the data times the Chew-Low factors for $\mu^2 \leq -t < 13\mu^2$ were fit to a straight line a+b(-t) and extrapolated to $t=\mu^2$. For the Durr-Pilkuhn method the data times the Durr-Pilkuhn factors for $\mu^2 < -t < 13\mu^2$ was averaged (fit to a constant). The results for the Chew-Low method are shown in Figure 31. The results for the Durr-Pilkuhn method are shown in Figure 32. We see that the contribution to Y_{22} and Y_{30} is negligible. It is assumed that the contribution to higher moments is also negligible. On the other hand Y_{21} is quite considerable indicating that there is natural parity exchange in the reaction $\pi^+ p \rightarrow \pi^+ p\pi^o$.

It was decided to follow Estabrooks et al.[17] in determining the various amplitudes. When only S and P waves are considered, the relationships between the spherical harmonics and the various waves are as follows:

$$\sqrt{4\pi}\, Y_{00} = |S|^2 + |P_0|^2 + |P_+|^2 + |P_-|^2$$

$$\sqrt{4\pi}\, Y_{10} = 2|S|\,|P_0| \cos\theta_{SP}.$$

$$\sqrt{4\pi}\, Y_{11} = \sqrt{2}\,|S|\,|P_-| \cos\theta_{SP}.$$

$$\sqrt{4\pi}\, Y_{20} = \frac{1}{\sqrt{5}}\left(2|P_0|^2 - |P_+|^2 - |P_-|^2\right)$$

$$\sqrt{4\pi}\, Y_{21} = \sqrt{\frac{6}{5}}\,|P_0|\,|P_{-1}| \cos\theta_{P_0P_-}$$

$$\sqrt{4\pi}\, Y_{22} = -\sqrt{\frac{3}{10}}\left(|P_+|^2 - |P_-|^2\right).$$

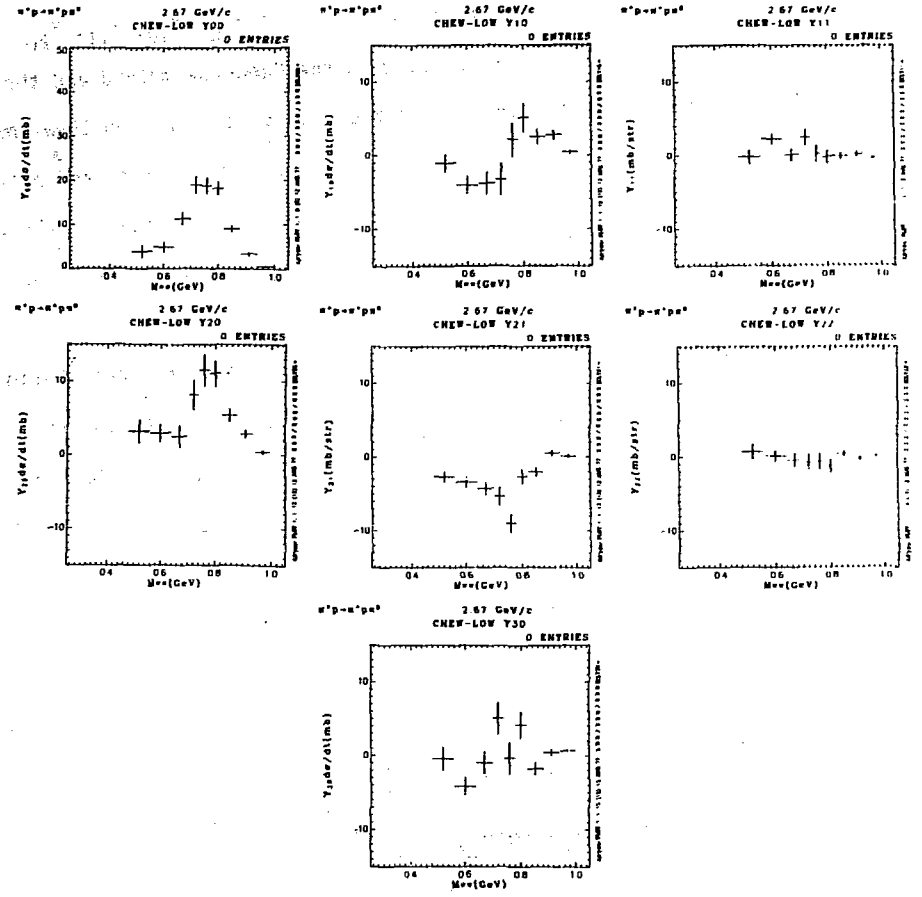

XBL 778 2711

Figure 31

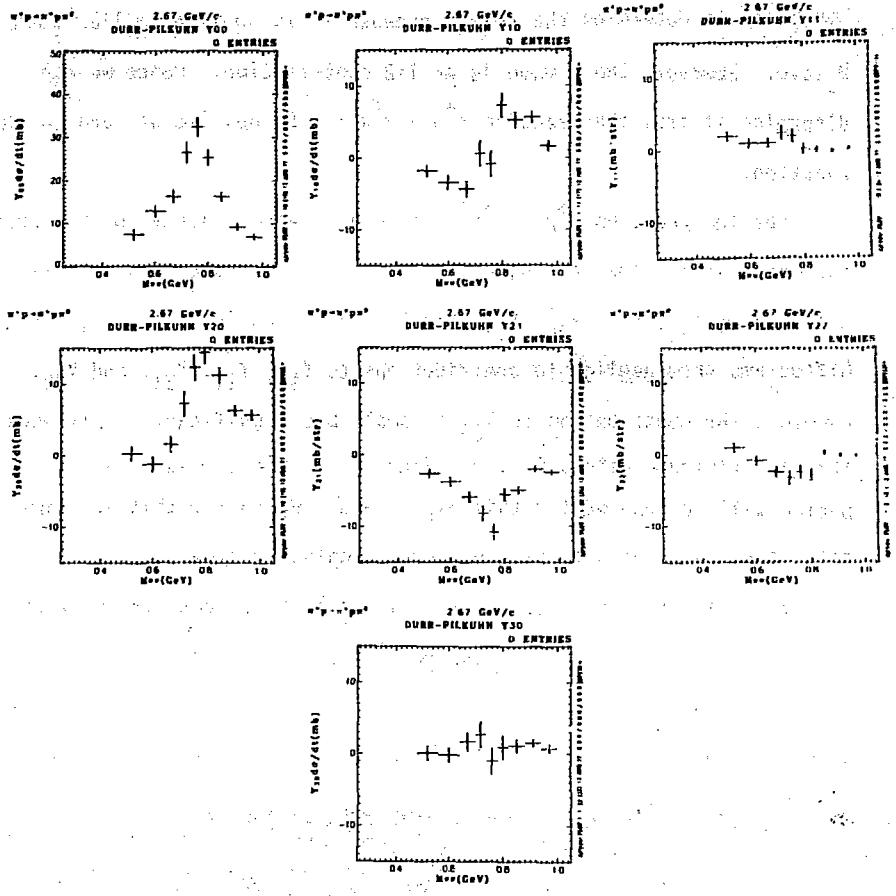
2.67 GeV/c
DURR-PILKUHN Y00
0 ENTRIES
2.67 GeV/c
DURR-PILKUHN Y10
0 ENTRIES
2.67 GeV/c
DURR-PILKUHN Y11
0 ENTRIES
2.67 GeV/c
DURR-PILKUHN Y20
0 ENTRIES
2.67 GeV/c
DURR-PILKUHN Y21
0 ENTRIES
2.67 GeV/c
DURR-PILKUHN Y22
0 ENTRIES
2.67 GeV/c
DURR-PILKUHN Y30
0 ENTRIES
Mππ(GeV)
XBL 778 2724

Figure 32

Since Y_{22} is negligible it is assumed that $|P_-| \cong |P_+|$. Y_{00} is too imprecise to determine the s-wave because it is so much smaller than the P wave. However, the s wave is an I=2 contribution. Hence we can determine it from the reaction $\pi^+p \to \pi^+\pi^+n$. So now let us turn to that reaction.

For the reaction $\pi^+p \to \pi^+\pi^+n$ the events were weighted by the spherical harmonics in the low -t region ($-t \leq 13\mu^2$). The histograms of these events weighted by Y_{10}, Y_{11}, Y_{20}, Y_{21}, and Y_{22} are shown in Figure 33. These histograms show negligible contributions to Y_{10}, Y_{11}, Y_{21}, and Y_{22}. However, the contribution to Y_{20} is small but significant. This indicates some interference with a D wave. Since it is small this D wave contribution will be ignored for this experiment. Hence for this experiment the total cross section will be considered completely s-wave.

So, the $\pi^+\pi^+$ cross section was extrapolated by both the Chew-Low method and the Durr-Pilkuhn method. In the $\pi^+\pi^+$ case the Durr-Pilkuhn results were to fit to a straight line (a+b(-t)) instead of a constant because the background was considerable. The results for these two methods are shown in Tables I and II.

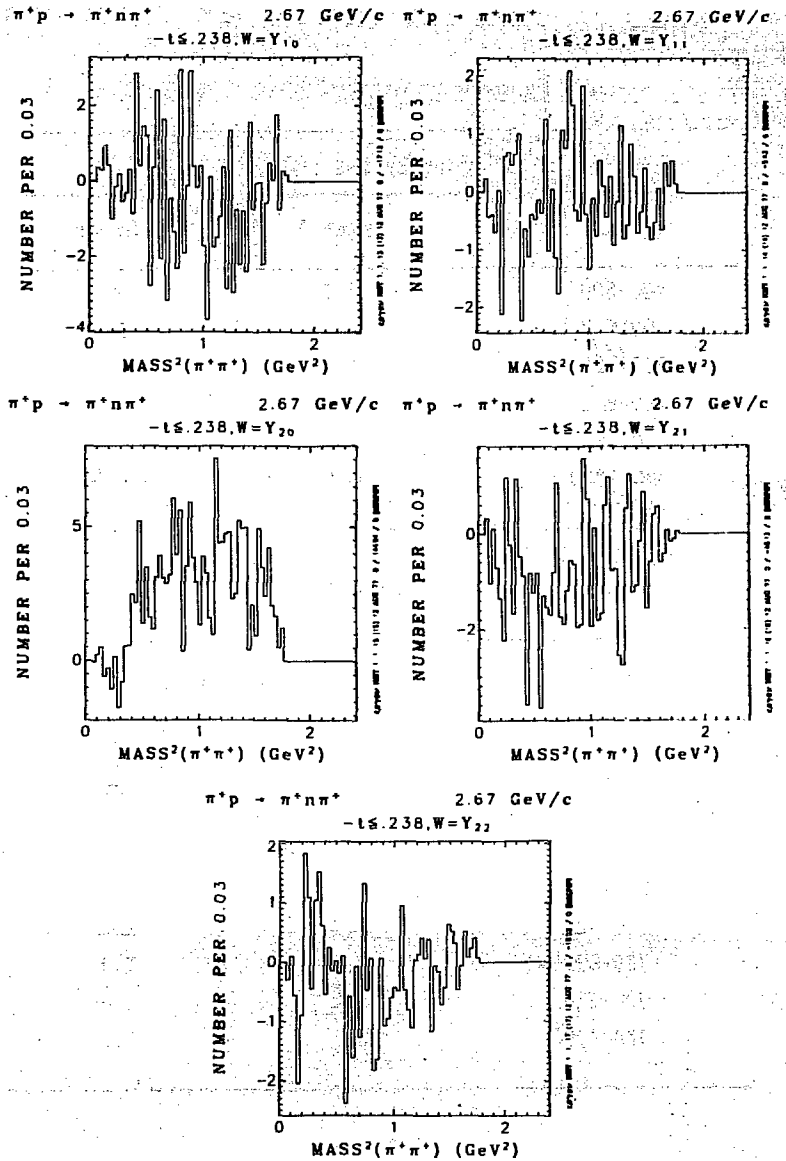

XBL 778-2721

Figure 33

Table I

$\pi^+\pi^+$ Scattering by the Chew-Low Method

ω(MeV)	σ(mb.)	error
400-500	4.0	3.6
500-620	6.4	2.1
620-720	8.1	1.8
720-820	5.9	1.3
820-920	5.9	1.1
920-1000	0.6	0.8

Table II

$\pi^+\pi^+$ Scattering by the Durr-Pilkuhn Method

ω(MeV)	σ(mb.)	error
400-500	-2.1	6.6
500-620	4.0	2.9
620-720	7.1	2.2
720-820	3.4	2.1
820-920	4.2	1.3
920-1000	-2.7	1.2

For the I=2 s-wave, Hyams et al.[14] use a scattering length formula:

$$T_0^2 = \frac{a_0 q}{1 - i a_0 q}$$

This gives a cross section:

$$\sigma_{\pi^+\pi^+} = 8\pi \ a_0^2/(1 + a_0^2 q^2)$$
$$\doteq 8\pi \ a_0^2$$

where the extra factor of two comes from Bose statistics. Hence in this experiment the middle four bins of Tables I and II were averaged. The extreme two bins were omitted because the errors were so large. This gives values of the cross section of:

Chew-Low

$$\sigma_{\pi^+\pi^+} = 6.575 \pm 0.815 \text{ mb.}$$

Durr-Pilkuhn

$$\sigma_{\pi^+\pi^+} = 4.67 \pm 1.09 \text{ mb.}$$

These values lead to the following values for $|a_0|$:

$$|a_0 \text{ Chew-Low}| = 0.115 \pm 0.007 \ m_{\pi^+}^{-1}$$

$$|a_0 \text{ Durr-Pilkuhn}| = 0.097 \pm 0.011 \ m_{\pi^+}^{-1}$$

in good agreement with the value used by Hyams et al.[14] of:

$$|a_0| = 0.1 \ m_\pi^{-1}.$$

The $\pi^+\pi^+$ data are of value for two reasons. One, they are of value to give an idea of the magnitude of the $\pi^+\pi^+$ cross section. The second reason is that they give the S-wave contribution which can be used in

conjuction with the $\pi^+\pi^o$ data to determine the P-wave contribution. If one attempts to determine the s-wave contribution from the $\pi^+\pi^o$ data, one finds that the result is lost in the noise.

Once the s-wave is known, P_o and P_- can be determined from the Estabrooks et al.[17] equations for Y_{00} and Y_{20}. These values are shown in Tables III and IV.

Table III

S and P Waves by the Chew-Low Method

w(MeV)	$\|S\|^2$(mb.)	$\|P_o\|^2$(mb.)	$\|P_-\|^2$(mb.)
480-560	6.575 ± .815	10.8 ± 4.2	-1.8 ± 2.5
560-640	6.575 ± .815	11.3 ± 3.5	-0.3 ± 2.1
640-700	6.575 ± .815	17.7 ± 4.4	7.9 ± 2.3
700-740	6.575 ± .815	41.8 ± 6.4	9.5 ± 2.9
740-780	6.575 ± .815	50.4 ± 6.9	4.8 ± 3.0
780-820	6.575 ± .815	48.5 ± 5.9	4.7 ± 2.4
820-880	6.575 ± .815	22.8 ± 3.2	1.4 ± 1.3
880-940	6.575 ± .815	9.3 ± 2.3	-2.0 ± 0.8
940-1000	6.575 ± .815	-0.5 ± 1.3	-2.0 ± 0.5

Table IV

S and P-Waves by the
Durr-Pilkuhn Method

w(MeV)	$\|S\|^2$(mb.)	$\|P_0\|^2$(mb.)	$\|P_-\|^2$(mb.)
480-560	4.67 ± 1.09	8.0 ± 2.4	6.9 ± 2.1
560-640	4.67 ± 1.09	10.2 ± 2.7	15.2 ± 2.2
640-700	4.67 ± 1.09	21.7 ± 3.4	15.6 ± 2.1
700-740	4.67 ± 1.09	48.9 ± 5.4	20.2 ± 2.8
740-780	4.67 ± 1.09	69.2 ± 5.8	20.5 ± 2.6
780-820	4.67 ± 1.09	66.3 ± 5.7	9.3 ± 2.1
820-880	4.67 ± 1.09	47.4 ± 3.6	2.8 ± 1.1
880-940	4.67 ± 1.09	25.8 ± 2.7	1.0 ± 0.7
940-1000	4.67 ± 1.09	21.5 ± 2.4	-0.9 ± 0.6

Now one may determine the cosines of the angles between the three waves by use of the equations for Y_{10}, Y_{11}, and Y_{21}. These cosines are given in Tables V and VI.

Table V

Cosines by the Chew-Low Method

w(MeV)	$\cos\theta_{SP_o}$	$\cos\theta_{SP_-}$	$\cos\theta_{P_oP_-}$	$\Delta\theta=\theta_{P_oP_-}-(\theta_{SP_o}+\theta_{SP_-})$
480-560	-.22 ± .45			
560-640	-.83 ± .37			
640-700	-.62 ± .28	+.03 ± .31	-1.17 ± .31	
700-740	-.35 ± .26	+.78 ± .36	-0.86 ± .25	0.78^o
740-780	+.21 ± .23	+.12 ± .35	-1.86 ± .25	
780-820	+.51 ± .21	-.09 ± .38	-.057 ± .30	-30.15^o
820-880	+.37 ± .16	-.10 ± .32	-1.14 ± .35	
880-940	+.63 ± .14			
940-1000				

Table VI

Cosines by the Durr-Pilkuhn Method

w(MeV)	$\cos\theta_{SP_0}$	$\cos\theta_{SP_-}$	$\cos\theta_{P_0P_-}$	$\Delta\theta=\theta_{P_0P_-}-(\theta_{SP_0}+\theta_{SP_-})$
480-560	-.52 ± 7.92	+.88 ± .25	-1.13 ± 3.12	
560-640	-.89 ± .34	+.29 ± .19	-0.97 ± .35	-32.20^0
640-700	-.77 ± .19	+.31 ± .19	-1.03 ± .13	
700-740	+.07 ± .19	+.63 ± .23	-0.84 ± .11	10.68^0
740-780	-.08 ± .17	+.51 ± .23	-0.93 ± .11	4.47^0
780-820	+.73 ± .15	+.09 ± .24	-0.72 ± .11	8.42^0
820-880	+.63 ± .12	+.05 ± .30	-1.39 ± .34	
880-940	+.91 ± .11	-.16 ± 1.24	-1.26 ± 2.25	
940-1000	+.29 ± .11			

The last column in Tables V and VI ($\Delta\theta$) gives a measure of the agreement between the three cosines. It seems that most of the time P_0 and P_- are almost 180^0 out of phase. Due to a lack of statistics, $\cos\theta_{P_0P_-}$ is often larger than -1. However, where the statistics are better, namely in the region of the ρ, there is fairly good agreement among the cosines particularly in the Durr-Pilkuhn method.

Now it would be nice to know the P-wave phase shifts. These can be found from the following:

$$|P_0|^2 = 12\pi\lambda^2|T|^2$$

$$= 12\pi\lambda^2\left(\frac{e^{2i\delta} - 1}{2i}\right)^2$$

$$= 3\pi\lambda^2(1 + \eta^2 - 2\eta\cos2\delta)$$

So:
$$\cos2\delta = \frac{1 + \eta^2 - (|P_0|^2/3\pi\lambda^2)}{2\eta}$$

Using the Durr-Pilkuhn method values for $|P_0|^2$ and using $\eta = .6$, which seems to best fit the data, we arrive at the values for δ given in Table VII. These values for the P-wave phase shift agree fairly well with those obtained by Estabrooks et al.[17]

Table VII

Phase Shifts by the Durr-Pilkuhn Method with $\eta = .6$

w(MeV)	cos2δ	δ
480-560	+1.032 ± .027	-
560-640	+ .972 ± .044	$7^0 \pm 5^0$
640-700	+ .658 ± .073	$24^0 \pm 3^0$
700-740	+ .003 ± .137	$45^0 \pm 4^0$
740-780	- .794 ± .167	$71^0 \pm 8^0$
780-820	- .875 ± .184	$104^0 \pm 11^0$
820-880	- .705 ± .133	$113^0 \pm 5^0$
880-940	- .003 ± .118	$135^0 \pm 3^0$
940-1000	- .095 ± .117	$132^0 \pm 3^0$

C. Conclusions and Comparisons

In conclusion the T=1 and T=2 $\pi\pi$ cross sections have been measured according to both the Chew-Low method and the Durr-Pilkuhn method. The T=2 total $\pi\pi$ cross sections turned out to be 6.575 ± 0.815 mb. by the Chew-Low method and 4.67 ± 1.09 mb. by the Durr-Pilkuhn method. Colton et al.[23] experimentally measured the T=2 elastic $\pi\pi$ cross section by the Durr-Pilkuhn method and found values in the range 7-11 mb. for several $\pi\pi$ mass ranges and two center of mass momenta. The reaction they used was $\pi^- p \rightarrow \pi^- \pi^- \Delta^{++}$. These values for the cross section are roughly in agreement with the values obtained in this experiment.

In the T=1 case the Durr-Pilkuhn method seems to give better values for the total $\pi\pi$ cross section than does the Chew-Low method. In this experiment the Durr-Pilkuhn method gives values that reach the unitary limit at the ρ peak whereas the Chew-Low method gives values that come up to only half the unitary limit.

A difference between the Durr-Pilkuhn method and the Chew-Low method is shown by Colton and Schlein.[24] They looked at the reaction $pp \rightarrow \Delta^{++} n$ and found that the Durr-Pilkuhn method gave better results for the reaction $\pi^+ p \rightarrow \Delta^{++} \rightarrow \pi^+ p$.

In an experiment by Jacques et al.[9] The Durr-Pilkuhn method gave results which reached the unitary limit for $\pi^- \pi^+ \rightarrow \rho^0 \rightarrow \pi^- \pi^-$ whereas when the Chew-Low method was used the results reached only half the unitary limit as in the present experiment.

Baton[25] used the Chew-Low method to determine the $\pi^- \pi^0$ cross section. He found the cross section to reach the unitary limit at the ρ peak contrary to the results in the present experiment and experiment cited above. There may have been some problem in his normalization.

So the Durr-Pilkuhn method seems to give values of the total $\pi\pi$ cross section that are more reasonable than those given by the Chew-Low method.

When the extrapolated angular distribution is examined it appears that there is considerable natural parity exchange in the reaction $\pi N \to \pi\pi N$. This can be seen from the fact that $|P_-|^2$ is considerable in relation to $|P_0|^2$. Therefore, the reaction does not go entirely by π exchange as we thought at first. Once the idea of total OPE in this reaction is dropped the Durr-Pilkuhn method of extrapolation seems to give more reasonable values for the extrapolated angular distribution as well as for the extrapolated cross sections than does the Chew-Low method, contrary to what seemed to be the case earlier.

The reasonableness of the values for the angular distribution can be seen by the agreement of the phase shifts with the results of Estabrooks et al.[17] An alternate method for finding the phase shifts or the width of the ρ is the colliding beam technique in which the interaction $e^+e^- \to \rho^0 \to \pi^+\pi^-$ is observed. An early experiment in 1969 by Auslender et al.[26] seemed to indicate the width of the ρ to be $\Gamma = 105 \pm 20$ MeV. This value was at variance with the values obtained by other methods. A later experiment, however by Benaksas et al.[27] in 1972 found a width $\Gamma = 149.6 \pm 23.2$ MeV after taking into account the ρ-ω interference which had been neglected by Auslender et al. This more recent value is in close agreement with the width obtained by other methods.

This agreement in angular distributions is pleasing from a theoretical point of view because the Durr-Pilkuhn method includes a more sophisticated idea of the distribuiton of events in the physical region than does the Chew-Low method and should be expected to give better extrapolated cross sections and angular distributions.

References

1. G. F. Chew, F. E. Low, Phys. Rev. 113, 1640 (1959).
2. J. M. Blatt, V. F. Weisskopf, Theoretical Nuclear Physics, John Wiley and Sons, Inc., p. 361 (1952).
3. H. P. Durr, H. Pilkuhn, Nuovo Cim. 40A, 899 (1965).
4. G. Wolf, Phys. Rev. Lett. 19, 925 (1967).
5. G. Laurens, π-π Scattering - 1973 (Tallahassee Conference), American Institute of Physics, p. 270 (1973).
6. S. Ciulli, Nuovo Cim. 61A, 787 (1969), 62A, 301 (1969).
7. R. E. Cutkosky, B. B. Deo, Phys. Rev. 174, 1859 (1969).
8. P. Baillon, π-π Scattering - 1973 (Tallahassee Conference), American Institute of Physics, p. 260 (1973).
9. P. Jacques, S. Barish, J. Bensinger, M. Hearn, W. Kononenko, E. M. O'Neill, W. Selove, π-π Scattering - 1973 (Tallahassee Conference), American Institute of Physics, p. 322 (1973).
10. G. Villet, M. David, R. Ayed, P. Bareyre, P. Borgeaud, J. Ernwein, J. Feltesse, Y. Lemoigne, P. Marty, A. V. Stirling, π-π Scattering - 1973 (Tallahassee Conference), American Institute of Physics, p. 307 (1973).
11. S. Toaff, J. C. Anderson, A. Engler, R. W. Kraemer, F. Weisser, J. Diaz, F. A. DiBianca, W. Fickinger, D. K. Robinson, C. A. Sullivan, π-π Scattering - 1973 (Tallahassee Conference), American Institute of Physics, p. 312 (1973).
12. G. Grayer, B. Hyams, C. Jones, P. Weilhammer, W. Blum, H. Dietl, W. Koch, E. Lorenz, G. Lutjens, W. Manner, J. Meissburger, U. Stierlin, W. Hoogland, π-π Scattering - 1973 (Tallahassee Conference) American Institute of Physics, p. 337 (1973).

13. E. W. Beier, π-π Scattering - 1973 (Tallahassee Conference), American Institute of Physics, p. 26 (1973).

14. B. Hyams, C. Jones, P. Weilhammer, W. Blum, H. Dietl, G. Grayer, W. Koch, E. Lorenz, G. Lutjens, W. Manner, J. Meissburger, W. Ochs, U. Stierlin, F. Wagner, π-π Scattering - 1973 (Tallahassee Conference), American Institue of Physics, p. 206 (1973).

15. W. Manner, Experimental Meson Spectroscopy - 1974 (Boston), American Institue of Physics, p. 22 (1974).

16. M. R. Pennington, π-π Scattering - 1973 (Tallahassee Conference), American Institute of Physics, p. 89 (1973).

17. P. Estabrooks, A. D. Martin, G. Grayer, B. Hyams, C. Jones, P. Weilhammer, W. Blum, H. Dietl, W. Koch, E. Lorenz, G. Lutjens, W. Manner, J. Meissburger, U. Stierlin, π-π Scattering - 1973 (Tallahassee Conference), American Institute of Physics, p. 37 (1973).

18. J. A. Charlesworth, R. L. Sekulin, M. J. Emms, J. B. Kinson, L. Riddiford, B. J. Stacey, M. F. Votruba, P. L. Woodworth, I. G. Bell, M. Dale, J. V. Major, π π Scattering - 1973 (Tallahassee Conference), American Institute of Physics, p. 317 (1973).

19. P. Estabrooks, A. D. Martin, π π Scattering - 1973 (Tallahassee Conference), American Institute of Physics, p. 357 (1973).

20. P. K. Williams, π-π Scattering - 1973(Tallahassee Conference), American Institue of Physics, p. 135 (1973).

21. G. Grayer, B. Hyams, C. Jones, P. Schlein, P. Weilhammer, W. Blum, H. Dietl, W. Koch, E. Lorenz, G. Lutjens, W. Manner, J. Meissburger, W. Ochs, U. Stierlin, π π Scattering - 1973 (Tallahassee Conference), American Institute of Physics, p. 117 (1973).

22. G. Gidal, G. Borreani, D. Grether, F. Lott, R. W. Birge, S. Y. Fung, W. Jackson, R. Poe, Phys. Rev. Lett. 23, 994 (1969).

23. E. Colton, E. Malamud, P. E. Schlein, A. D. Johnson, V. J. Stenger, P. G. Wohlmut, Phys. Rev. 3D, 2028 (1971).

24. E. Colton, P. E. Schlein, University of California at Los Angeles report, UCLA-1039 (1969).

25. J. P. Baton, Centre d'Études Nucléaires de Saclay report CEA-R-3543 (1969).

26. V. L. Auslender, G. I. Budker, E. V. Pakhtusova, Yu. N. Pestov, V. A. Sidorov, A. N. Skrinskii, A. G. Khabakhpashev, Sov. J. Nucl. Phys. 9, 69 (1969).

27. D. Benaksas, G. Cosme, B. Jean-Marie, S. Jullian, F. LaPlanche, J. LeFrancois, A. D. Liberman, G. Parrour, J. P. Repellin, G. Sauvage, Phys. Lett. 39B, 289 (1972).